Highly Stable Novel Inorganic Hydrides

Randell L. Mills

BlackLight Power, Inc.
493 Old Trenton Road
Cranbury, NJ 08512
USA

Novel inorganic hydride compounds $KH\,KHCO_3$ and KH were isolated following the electrolysis of a K_2CO_3 electrolyte. The compounds which comprised high binding energy hydride ions were stable in water, and KH was stable at elevated temperature (600 °C). Inorganic hydride clusters $K[KH\,KHCO_3]_n^+$ were identified by positive Time of Flight Secondary Ion Mass Spectroscopy (ToF-SIMS) of $KH\,KHCO_3$. The negative ToF-SIMS was dominated by hydride ion. The positive and negative ToF-SIMS of KH showed essentially K^+ and H^- only, respectively. Moreover, the existence of novel hydride ions was determined using X-ray photoelectron spectroscopy, and proton nuclear magnetic resonance spectroscopy. Hydride ions with increased binding energies may be the basis of a high voltage battery for electric vehicles.

INTRODUCTION

Evidence of the changing landscape for automobiles can be found in the recent increase in research into the next generation of automobiles. But, the fact that there is no clear front-runner in the technological race to replace the internal combustion (IC) engine can be attested to by the divergent approaches taken by the major automobile companies. Programs include various approaches to hybrid vehicles, alternative fueled vehicles such as dual-fired engines that can run on gasoline or compressed natural gas, and a natural gas-fired engine. Serious efforts are also being put into a number of alternative fuels such as ethanol, methanol, propane, and reformulated gasoline. To date, the most favored approach is an electric vehicle based on fuel cell technology or advanced battery technology such as sodium nickel chloride, nickel-metal hydride, and lithium-ion batteries [1]. Although billions of dollars are being spent to develop an alternative to the IC engine, there is no technology in sight that can match the specifications of an IC engine system [2].

Fuel cells have advantages over the IC engine because they convert hydrogen to water at about 70% efficiency when running at about 20% below peak output [3]. But, hydrogen is difficult and dangerous to store. Cryogenic, compressed gas, and metal hydride storage are the main options. In the case of cryogenic storage, liquefaction of hydrogen requires an amount of electricity which is at least 30% of the lower heating value of liquid hydrogen [4]. Compressed hydrogen, and metal hydride storage are less viable since the former requires an unacceptable volume, and the latter is heavy and has difficulties supplying hydrogen to match a load such as a fuel cell [4]. The main challenge with hydrogen as a replacement to gasoline is that a hydrogen production and refueling infrastructure would have to be built. Hydrogen may be obtained by reforming fossil fuels. However, in practice fuel cell vehicles would probably achieve only 10 to 45 percent efficiency because the process of reforming fossil fuel into hydrogen and carbon dioxide requires energy [3]. Presently, fuel cells are also impractical due to their high cost as well as the lack of inexpensive reforming technology [5].

In contrast, batteries are attractive because they can be recharged wherever electricity exists which is ubiquitous. The cost of mobile

energy from a battery powered car may be less than that from a fossil fuel powered car. For example, the cost of energy per mile of a nickel metal hydride battery powered car is 25% of that of a IC powered car [6]. However, current battery technology is trying to compete with something that it has little chance of imitating. Whichever battery technology proves to be superior, no known electric power plant will match the versatility and power of an internal combustion engine. A typical IC engine yields more than 10,000 watt-hours of energy per kilogram of fuel, while the most promising battery technology yields 200 watt-hours per kilogram [2].

A high voltage battery would have the advantages of much greater power and much higher energy density. The limitations of battery chemistry may be attributed to the binding energy of the anion of the oxidant. For example, the 2 volts provided by a lead acid cell is limited by the $1.46\,eV$ electron affinity of the oxide anion of the oxidant PbO_2. An increase in the oxidation state of lead such as $Pb^{2+} \rightarrow Pb^{3+} \rightarrow Pb^{4+}$ is possible in a plasma. Further oxidation of lead could also be achieved in theory by electrochemical charging. However, higher lead oxidation states are not achievable because the oxide anion required to form a neutral compound would undergo oxidation by the highly oxidized lead cation. An anion with an extraordinary binding energy is required for a high voltage battery. One of the highest voltage batteries known is the lithium fluoride battery with a voltage of about 6 volts. The voltage can be attributed to the higher binding energy of the fluoride ion. The electron affinity of halogens increases from the bottom of the Group VII elements to the top. Hydride ion may be considered a halide since it possess the same electronic structure. And, according to the binding energy trend, it should have a high binding energy. However, the binding energy is only $0.75\,eV$ which is much lower than the $3.4\,eV$ binding energy of a fluoride ion.

Novel inorganic hydride compounds having the formula $KH\,KHCO_3$ and KH were isolated from an aqueous K_2CO_3 electrolytic cell reactor. KH was stable at elevated temperature (600 °C). Inorganic hydride clusters $K[KH\,KHCO_3]_n^+$ were identified by positive Time of Flight Secondary Ion Mass Spectroscopy (ToF-SIMS) of $KH\,KHCO_3$. The negative ToF-SIMS was dominated by hydride ion. The positive and negative ToF-

SIMS of KH showed essentially K^+ and H^- only, respectively. A hydride ion with a binding energy of $22.8\,eV$ has been observed by X-ray photoelectron spectroscopy (XPS) of $KH\,KHCO_3$ having upfield shifted solid state magic-angle spinning proton nuclear magnetic resonance (^1H MAS NMR) peaks. Moreover, a polymeric structure is indicated by Fourier transform infrared (FTIR) spectroscopy. Hydride ions with a binding energies of $22.8\,eV$ and $69.2\,eV$ have been observed by XPS of KH. The discovery of novel hydride ions with high binding energies has implications for a new field of hydride chemistry with applications such as a high voltage battery. Such extremely stable hydride ions may stabilize positively charged ions in an unprecedented highly charged state. A battery may be possible having projected specifications that surpass those of the internal combustion engine.

Hydride ions having extraordinary binding energies may stabilize a cation M^{x+} in an extraordinarily high oxidation state such as +2 in the case of lithium. Thus, these hydride ions may be used as the basis of a high voltage battery of a rocking chair design wherein the hydride ion moves back and forth between the cathode and anode half cells during discharge and charge cycles. Exemplary reactions for a cation M^{x+} are:

Cathode reaction:

$$MH_x + e^- \rightarrow MH_{x-1} + H^- \qquad (1)$$

Anode reaction:

$$MH_{x-2} + H^- \rightarrow MH_{x-1} + e^- \qquad (2)$$

Overall reaction:

$$MH_x + MH_{x-2} \rightarrow 2MH_{x-1} \qquad (3)$$

EXPERIMENTAL

Synthesis

A. Potassium Hydride Potassium Hydrogen Carbonate, $KH\,KHCO_3$, Synthesis with an Electrolytic Cell

An electrolytic cell comprising a K_2CO_3 electrolyte, a nickel wire cathode, and platinized titanium anodes was used to synthesize the $KH\,KHCO_3$ sample [7]. Briefly, the cell vessel comprised a 10 gallon (33 in. x 15 in.) Nalgene tank. An outer cathode comprised 5000 meters of 0.5 mm diameter clean, cold drawn nickel wire (NI 200 0.0197", HTN36NOAG1, A-1 Wire Tech, Inc., 840-39th Ave., Rockford, Illinois, 61109) wound on a polyethylene cylindrical support. A central cathode comprised 5000 meters of the nickel wire wound in a toroidal shape. The central cathode was inserted into a cylindrical, perforated polyethylene container that was placed inside the outer cathode with an anode array between the central and outer cathodes. The anode comprised an array of 15 platinized titanium anodes (ten - Engelhard Pt/Ti mesh 1.6" x 8" with one 3/4" by 7" stem attached to the 1.6" side plated with 100 U series 3000; and 5 - Engelhard 1" diameter x 8" length titanium tubes with one 3/4" x 7" stem affixed to the interior of one end and plated with 100 U Pt series 3000). Before assembly, the anode array was cleaned in 3 M HCl for 5 minutes and rinsed with distilled water. The cathode was cleaned by placing it in a tank of 0.57 M K_2CO_3/3% H_2O_2 for 6 hours and then rinsing it with distilled water. The anode was placed in the support between the central and outer cathodes, and the electrode assembly was placed in the tank containing electrolyte. The electrolyte solution comprised 28 liters of 0.57 M K_2CO_3 (Alfa K_2CO_3 99%). Electrolysis was performed at 20 amps constant current with a constant current (± 0.02%) power supply.

Samples were isolated from the electrolytic cell by concentrating the K_2CO_3 electrolyte about six fold using a rotary evaporator at 50 °C until a yellow white polymeric suspension formed. Precipitated crystals of the suspension were then grown over three weeks by allowing the saturated solution to stand in a sealed round bottom flask at 25°C.

Control samples utilized in the following experiments contained K_2CO_3 (99%), $KHCO_3$ (99.99%), HNO_3 (99.99%), and KH (99%).

B. Potassium Hydrino Hydride, KH, Synthesis with an Electrolytic Cell

An electrolytic cell comprising a K_2CO_3 electrolyte, a nickel wire cathode, and platinized titanium anodes described by Mills et al. [7] was used to synthesize potassium hydride, KH. The cell was equivalent to that described above except that it lacked the additional central cathode.

After 3 months of operation, the cathode wire obtained a graphite colored coating. The cathode was placed in 10 gallon (33 in. x 15 in.) Nalgene tank of 0.57 M K_2CO_3/3% H_2O_2 for 6 hours. A very vigorous exothermic reaction was observed during the six hours. The cathode was removed and placed in a second 10 gallon (33 in. x 15 in.) Nalgene tank of distilled water. NiO was observed to precipitate in the tank containing 0.57 M K_2CO_3/3% H_2O_2. The coat was observed to be removed from the cathode when it was pulled from the distilled water bath. A white polymeric solid floated to the top of the water bath over 2 weeks. The solid was collected by scooping it with a 250 ml beaker. The polymeric material was stable in water indefinitely (over a year with no observable change). The material was pure white and appeared like cotton suspended in water. Other samples were obtained which were thin films. The density was less than that of water. The material was observed to be weakly ferromagnetic. It collapsed along the magnet field lines and was attracted to a magnet in solution. It could be pulled out of water with a strong magnet. It was poured onto an evaporation dish, dried, and analyzed.

ToF-SIMS Characterization

The crystalline samples were sprinkled onto the surface of double-sided adhesive tapes and characterized using a Physical Electronics TFS-2000 ToF-SIMS instrument. The primary ion gun utilized a $^{69}Ga^+$ liquid metal source. In order to remove surface contaminants and expose a fresh surface, the samples were sputter cleaned for 30 seconds using a $40\mu m$ X $40\mu m$ raster. The aperture setting was 3, and the ion current was 600 pA resulting in a total ion dose of 10^{15} $ions/cm^2$.

During acquisition, the ion gun was operated using a bunched (pulse width 4 ns bunched to 1 ns) 15 kV beam [8-9]. The total ion dose was 10^{12} *ions* / cm^2. Charge neutralization was active, and the post accelerating voltage was 8000 V. Three different regions on each sample of $(12\mu m)^2$, $(18\mu m)^2$, and $(25\mu m)^2$ were analyzed. The positive and negative SIMS spectra were acquired. Representative post sputtering data is reported.

XPS Characterization

A series of XPS analyses were made on the crystalline samples each mounted on a silicon wafer using a Scienta 300 XPS Spectrometer. The fixed analyzer transmission mode and the sweep acquisition mode were used. A survey spectrum was obtained over the region $E_b = 0\ eV$ to $1200\ eV$. The primary element peaks allowed for the determination of all of the elements present in each sample isolated from the K_2CO_3 electrolyte. The survey spectrum also detected shifts in the binding energies of potassium and oxygen which had implications as to the identity of the compound containing the elements. A high resolution XPS spectrum was also obtained of the low binding energy region ($E_b = 0\ eV$ to $100\ eV$) to determine the presence of novel XPS peaks. The step energy in the survey scan was $0.5\ eV$, and the step energy in the high resolution scan was $0.15\ eV$. In the survey scan, the time per step was 0.4 seconds, and the number of sweeps was 4. In the high resolution scan, the time per step was 0.3 seconds, and the number of sweeps was 30. $C\ 1s$ at $284.6\ eV$ was used as the internal standard.

NMR Spectroscopy

^1H MAS NMR was performed on the crystalline samples. The data were obtained on a custom built spectrometer operating with a Nicolet 1280 computer. Final pulse generation was from a tuned Henry radio amplifier. The ^1H NMR frequency was 270.6196 MHz. A $2\ \mu$sec pulse corresponding to a 15° pulse length and a 3 second recycle delay were used. The window was $\pm 31\ kHz$. The spin speed was 4.5 kHz. The number of scans was 1000. The offset was 1527.12 Hz, and the magnetic flux was 6.357 T. Chemical shifts were referenced to external TMS.

FTIR Spectroscopy

Samples were transferred to an infrared transmitting substrate and analyzed by FTIR spectroscopy using a Nicolet Magna 550 FTIR Spectrometer with a NicPlan FTIR microscope. The number of scans was 500 for both the sample and background. The number of background scans was 500. The resolution was 8.000. A dry air purge was applied.

Thermal Decomposition with Analysis by Mass Spectroscopy

Mass spectroscopy was performed on the gases released from the thermal decomposition of the samples. One end of a 4 mm ID fritted capillary tube containing about 5 mg of sample was sealed with a 0.25 in. Swagelock union and plug (Swagelock Co., Solon, OH). The other end was connected directly to the sampling port of a Dycor System 1000 Quadrapole Mass Spectrometer (Model D200MP, Ametek, Inc., Pittsburgh, PA with a HOVAC Dri-2 Turbo 60 Vacuum System). The capillary was heated with a Nichrome wire heater wrapped around the capillary. The mass spectrum was obtained at the ionization energy of 70 eV at a sample temperature of 600 °C with the detection of hydrogen indicated by a $m/e=2$ peak.

The control hydrogen gas was ultrahigh purity (MG Industries).

RESULTS AND DISCUSSION

ToF-SIMS

A. ToF-SIMS of Potassium Hydride Potassium Hydrogen Carbonate, *KH KHCO*$_3$, Electrolytic Cell Sample

The positive ToF-SIMS spectrum obtained from the $KHCO_3$ control is shown in Figures 1 and 2. In addition, the positive ToF-SIMS of a sample isolated from the electrolytic cell is shown in Figures 3 and 4. The respective hydride compounds and mass assignments appear in Table 1. In both the control and electrolytic samples, the positive ion spectrum are dominated by the K^+ ion. Two series of positive ions $\{K[K_2CO_3]_n^+ \ m/z=(39+138n)$ and $K_2OH[K_2CO_3]_n^+ \ m/z=(95+138n)\}$ are observed in the $KHCO_3$ control. Other peaks containing potassium include

KC^+, $K_xO_y^+$, $K_xO_yH_z^+$, KCO^+, and K_2^+. However, in the electrolytic cell sample, three new series of positive ions are observed at $\{K[KH\,KHCO_3]_n^+ \; m/z=(39+140n)$, $K_2OH[KH\,KHCO_3]_n^+ \; m/z=(95+140n)$, and $K_3O[KH\,KHCO_3]_n^+ \; m/z=(133+140n)\}$. These ions correspond to inorganic clusters containing novel hydride combinations (i.e. $KH\,KHCO_3$ units plus other positive fragments).

The comparison of the positive ToF-SIMS spectrum of the $KHCO_3$ control with the electrolytic cell sample shown in Figures 1-2 and 3-4, respectively, demonstrates that the $^{39}K^+$ peak of the electrolytic cell sample may saturate the detector and give rise to a peak that is atypical of the natural abundance of ^{41}K. The natural abundance of ^{41}K is 6.7%; whereas, the observed ^{41}K abundance from the electrolytic cell sample is 57%. This atypical abundance was also confirmed using ESIToFMS [10]. The high resolution mass assignment of the $m/z=41$ peak of the electrolytic sample was consistent with ^{41}K, and no peak was observed at $m/z=42.98$ ruling out $^{41}KH_2^+$. Moreover, the natural abundance of ^{41}K was observed in the positive ToF-SIMS spectra of $KHCO_3$, KNO_3, and KI standards that were obtained with an ion current such that the ^{39}K peak intensity was an order of magnitude higher than that given for the electrolytic cell sample. The saturation of the ^{39}K peak of the positive ToF-SIMS spectrum by the electrolytic cell sample is indicative of a unique crystalline matrix [11].

The negative ToF-SIMS spectrum ($m/e=0-50$) of the $KHCO_3$ (99.99%) sample and the negative ToF-SIMS spectrum ($m/e=0-30$) of the electrolytic cell sample are shown in Figures 5 and 6, respectively. The negative ion ToF-SIMS of the electrolytic cell sample was dominated by H^-, O^-, and OH^- peaks. A series of nonhydride containing negative ions $\{KCO_3[K_2CO_3]_n^- \; m/z=(99+138n)\}$ was also present which implies that H_2 was eliminated from $KH\,KHCO_3$ during fragmentation of the compound $KH\,KHCO_3$. Comparing the H^- to O^- ratio of the electrolytic cell sample to that of the $KHCO_3$ control sample, the H^-peak was about an order of magnitude higher in the electrolytic cell sample.

B. ToF-SIMS of Potassium Hydrino Hydride, KH, Electrolytic Cell Sample

The positive ToF-SIMS spectrum obtained from the KH electrolytic cell sample is shown in Figure 7. The positive spectrum was dominated by the potassium peak K^+ $m/z=39$ followed by the proton peak. Small silicon, sodium, and hydrocarbon fragment peaks such as C_2H_3 $m/z=27$ and C_2H_5 $m/z=29$, K_2^+ $m/z=87$, $K(KO)^+$ $m/z=94$, and $K(KOH)^+$ $m/z=95$ were also observed.

The positive spectrum of the $KHCO_3$ control shown in Figures 1 and 2 was also dominated by the potassium peak K^+ $m/z=39$. Two series of positive ions $\{K[K_2CO_3]_n^+$ $m/z=(39+138n)$ and $K_2OH[K_2CO_3]_n^+$ $m/z=(95+138n)\}$ were observed in the $KHCO_3$ control. Other peaks containing potassium included KC^+ $m/z=51$, $K_xO_y^+$, $K_xO_yH_z^+$, KCO^+ $m/z=67$, and K_2^+ $m/z=78$.

The negative ion ToF-SIMS of KH shown in Figure 8 was dominated by H^-. O^- $m/z=16$ and OH^- $m/z=17$ dominated the negative ion ToF-SIMS of the $KHCO_3$ control as shown in Figure 5. These peaks were present in the case of KH, but they were very small in comparison to the $KHCO_3$ control. For both samples smaller hydrocarbon fragment peaks such as C^- $m/z=12$ and CH^- $m/z=13$ were observed. A series of negative ions $\{KCO_3[K_2CO_3]_n^-$ $m/z=(99+138n)\}$ was also present in the control which were not observed in the KH sample. A hydride peak probably due to OH^- $m/z=17$ which was significantly smaller than the O^- $m/z=16$ peak was observed in the control.

XPS

A. XPS of Potassium Hydride Potassium Hydrogen Carbonate, $KH\,KHCO_3$, Electrolytic Cell Sample

The 0 to 80 eV binding energy region of a high resolution XPS spectrum of the $KH\,KHCO_3$ electrolytic cell sample is shown in Figure 9. The XPS survey spectrum the $KH\,KHCO_3$ electrolytic cell sample with the primary elements identified is shown in Figure 10. No elements were present in the survey scans which can be assigned to peaks in the low binding energy region with the exception of a small variable contaminant

of sodium at 63 eV and 31 eV, potassium at 16.2 eV and 32.1 eV, and oxygen at 23 eV. Accordingly, any other peaks in this region must be due to novel species. The $K\,3s$ and $K\,3p$ are shown in Figure 9 at 16.2 eV and 32.1 eV, respectively. A weak $Na\,2s$ is observed at 63 eV. The $O\,2s$ which is weak compared to the potassium peaks of K_2CO_3 is typically present at 23 eV, but is broad or obscured in Figure 9.

Peaks centered at 22.8 eV and 38.8 eV which do not correspond to any other primary element peaks were observed. The intensity and shift match shifted $K\,3s$ and $K\,3p$. Hydrogen is the only element which does not have primary element peaks; thus, it is the only candidate to produce the shifted peaks. These peaks may be shifted by a highly binding hydride ion with a binding energy of 22.8 eV given in the Appendix that bonds to potassium $K\,3p$ and shifts the peak to this energy. In this case, the $K\,3s$ is similarly shifted. These peaks were not present in the case of the XPS of matching samples isolated from an identical electrolytic cell except that Na_2CO_3 replaced K_2CO_3 as the electrolyte.

XPS further confirmed the ToF-SIMS data by showing shifts of the primary elements. The splitting of the principal peaks of the survey XPS spectrum is indicative of multiple forms of bonding involving the atom of each split peak. For example, the XPS survey spectrum shown in Figure 10 shows extraordinary potassium and oxygen peak shifts. All of the potassium primary peaks are shifted to about the same extent as that of the $K\,3s$ and $K\,3p$. In addition, extraordinary $O\,1s$ peaks of the electrolytic cell sample were observed at 537.5 eV and 547.8 eV; whereas, a single $O\,1s$ was observed in the XPS spectrum of K_2CO_3 at 532.0 eV. The results are not due to uniform charging as the internal standard $C\,1s$ remains the same at 284.6 eV. The results are not due to differential charging because the peak shapes of carbon and oxygen are normal, and no tailing of these peaks was observed. The binding energies of the K_2CO_3 control and the $KH\,KHCO_3$ electrolytic cell sample are shown in Table 2. The range of binding energies from the literature [12] for the peaks of interest are given in the final row of Table 2. The $K\,3p$, $K\,3s$, $K\,2p_{3/2}$, $K\,2p_{1/2}$, and $K\,2s$ XPS peaks and the $O\,1s$ XPS peaks shifted to an extent greater than those of known compounds may correspond to and identify $KH\,KHCO_3$.

B. XPS of Poly-Potassium Hydrino Hydride, *KH*, Electrolytic Cell Sample

The XPS survey scan of the *KH* electrolytic cell sample is shown in Figure 11. *C* 1*s* at 284.5 *eV* was used as the internal standard for the *KH* sample and the control K_2CO_3. The major species present in the control are potassium and carbon and oxygen. The major species present in the *KH* sample was potassium. Large silicon, oxygen and graphitic and hydrocarbon carbon peaks were also seen that originated from the silicon wafer sample mount. Nitrogen was present, and trace magnesium and sodium may be present. The identifying peaks of the primary elements and their binding energies are: *Na* 1*s* at 1072.2 eV, *O* 1*s* at 532.0 eV, *Na* $KL_{23}L_{23}$ at 496.6 eV, *N* 1*s* at 399.3 eV, *K* 2*s* at 377.2 eV, *Mg* $KL_{23}L_{23}$ at 305.9 eV, *K* $2p_{1/2}$ at 295.4 eV, *K* $2p_{3/2}$ at 292.5 eV, *C* 1*s* at 285.5 and 284.6 eV, *Si* $2p_{3/2}$ at 156.7 eV and 153.4 eV, *Si* 2*s* at 105.7 eV and 102.1 eV, and *Mg* 2*s* at 88.5 eV.

No elements were present in the survey scan which could be assigned to peaks in the low binding energy region with the exception of the *K* 3*p* at 16.8 eV, *K* 3*s* at 33.0 eV, *O* 2*s* at 26.2 eV, and *Mg* 2*p* at 49.6 eV. Accordingly, any other peaks in this region must be due to novel species. The 0-80 eV binding energy region of a high resolution XPS spectrum of the *KH* electrolytic cell sample is shown in Figure 12. Peaks of interest were observed in the valance band at 3.8 eV, 9.95 eV, and 13.7 eV which may be due to nitrogen, carbon, and oxygen, but the assignment can not be made with certainty. A 62.8 peak may be assigned to *Na* 2*s*. However, no peak is detectable above baseline at 29.8 eV which corresponds to *Na* $2p_{1/2}$. Since the intensity of the *Na* $2p_{1/2}$ peak is less than *Na* 2*s*, and the *Na* 2*s* peak is weak, the *Na* $2p_{1/2}$ may not be seen. So, the assignment is uncertain. Novel peaks were observed in the *KH* sample at 19.5 eV, 36.0 eV, and 68.0 eV. The 68.0 eV peak may be assigned to *Ni* 3*p*, but the shape is incorrect. And, if the *Ni* $2p_{3/2}$ at about 860 eV is present, it is smaller than the proposed *Ni* 3*p*. Thus, the 68.0 eV can not be assigned to *Ni* 3*p*.

The XPS peaks at 19.5 eV, 36.0 eV, and 68.0 eV do not correspond to any other primary element peaks. The 68.0 eV peak may correspond to a hydride ion with a binding energy of 69.2 *eV* given in the Appendix. Peaks at 19.5 eV and 36.0 eV which do not correspond to any other

primary element peaks were observed. The intensity and shift match shifted $K\,3s$ and $K\,3p$. Hydrogen is the only element which does not have primary element peaks; thus, it is the only candidate to produce the shifted peaks. These peaks may be shifted by a highly binding hydride ion with a binding energy of $22.8\,eV$ given in the Appendix that bonds to potassium $K\,3p$ and shifts the peak to this energy. In this case, the $K\,3s$ is similarly shifted. The shift of about 3 eV is greater than that of known potassium compounds. These peaks were not present in the case of the XPS of matching samples isolated from an identical electrolytic cell except that Na_2CO_3 replaced K_2CO_3 as the electrolyte.

The KH electrolytic cell sample was observed to be weakly ferromagnetic. The origin of the magnetism is from nonmetallic elements which were most likely potassium and hydrogen.

NMR

The signal intensities of the ^1H MAS NMR spectrum of the K_2CO_3 reference were relatively low. It contained a water peak at 1.208 ppm, a peak at 5.604 ppm, and very broad weak peaks at 13.2 ppm, and 16.3 ppm. The ^1H MAS NMR spectrum of the $KHCO_3$ reference contained a large peak at 4.745 with a small shoulder at 5.150 ppm, a broad peak at 13.203 ppm, and small peak at 1.2 ppm.

The ^1H MAS NMR spectra of the $KH\,KHCO_3$ electrolytic cell sample is shown in Figure 13. The peak assignments are given in Table 3. The reproducible peaks assigned to $KH\,KHCO_3$ in Table 3 were not present in the controls except for the peak assigned to water at +5.066 ppm. The novel peaks could not be assigned to hydrocarbons. Hydrocarbons were not present in the electrolytic cell sample based on the TOFSIMS spectrum and FTIR spectra which were also obtained (see below). The novel peaks without identifying assignment are consistent with $KH\,KHCO_3$. The NMR peak of the hydride ion of potassium hydride was observed at 0.8 and 1.1 ppm relative to TMS. The upfield peaks of Figure 13 are assigned to novel hydride ion ($KH-$) in different environments. The down field peaks are assigned to the proton of the potassium hydrogen carbonate species in different chemical environments ($-KHCO_3$).

FTIR

The FTIR spectra of K_2CO_3 (99%) and $KHCO_3$ (99.99%) were compared with that of the $KH\,KHCO_3$ electrolytic cell sample. A spectrum of a mixture of the bicarbonate and the carbonate was produced by digitally adding the two reference spectra. The two standards alone and the mixed standards were compared with that of the electrolytic cell sample. From the comparison, it was determined that the electrolytic cell sample contained potassium carbonate but did not contain potassium bicarbonate. The unknown component could be a bicarbonate other than potassium bicarbonate. The spectrum of potassium carbonate was digitally subtracted from the spectrum of the electrolytic cell sample. Several bands were observed including bands in the $1400-1600\ cm^{-1}$ region. Some organic nitrogen compounds (e.g. acrylamides, pyrolidinones) have strong bands in the region $1660\ cm^{-1}$ [13]. However, the lack of any detectable $C-H$ bands ($\approx 2800-3000\ cm^{-1}$) and the bands present in the 700 to $1100\ cm^{-1}$ region indicate an inorganic material [14]. Peaks are not assignable to potassium carbonate were observed at 3294, 3077, 2883, $1100\ cm^{-1}$, 2450, 1660, 1500, 1456, 1423, 1300, 1154, 1023, 846, 761, and $669\ cm^{-1}$.

The overlap FTIR spectrum of the electrolytic cell sample and the FTIR spectrum of the reference potassium carbonate appears in Figure 14. In the 700 to $2500\ cm^{-1}$ region, the peaks of the electrolytic cell sample closely resemble those of potassium carbonate, but they are shifted about $50\ cm^{-1}$ to lower frequencies. The shifts are similar to those observed by replacing potassium (K_2CO_3) with rubidium (Rb_2CO_3) as demonstrated by comparing their IR spectra [15]. The shifted peaks may be explained by a polymeric structure for the compound $KH\,KHCO_3$ identified by ToF-SIMS, XPS, and NMR.

Mass Spectroscopy (MS)

The *KH* electrolytic cell sample did not decompose upon heating to 600 °C. Essentially no hydrogen was observed by mass spectroscopy. The sample changed very little which indicates no decomposition and extraordinary stability for a compound mainly comprised of hydrogen.

Further Analytical Tests

X-ray diffraction (XRD), elemental analysis using inductively coupled plasma (ICP), and Raman spectroscopy were also performed on the $KH\,KHCO_3$ electrolytic sample [10]. The XRD data indicated that the diffraction pattern of the electrolytic cell sample does not match that of either KH, $KHCO_3$, K_2CO_3, or KOH. The elemental analysis supports $KH\,KHCO_3$. In addition to the known Raman peaks of $KHCO_3$ and a small peak assignable to K_2CO_3, unidentified peaks at $1685\,cm^{-1}$ and $835\,cm^{-1}$ were present. Work in progress [10] demonstrates that $KH\,KHCO_3$ may also be formed by a reaction of gaseous KI with atomic hydrogen in the presence of K_2CO_3 [16]. In addition to the previous analytical studies, the fragment $KK_2CO_3^+$ corresponding to $KH\,KHCO_3$ was observed by electrospray ionization time of flight mass spectroscopy as a chromatographic peak on a C18 liquid chromatography column typically used to separate organic compounds. No chromatographic peaks were observed in the case of inorganic compound controls KI, $KHCO_3$, K_2CO_3, and KOH

DISCUSSION

Alkali and alkaline earth hydrides react violently with water to release hydrogen gas which subsequently ignites due to the exothermic reaction with water. Typically metal hydrides decompose upon heating at a temperature well below the melting point of the parent metal. These saline hydrides, so called because of their saltlike or ionic character, are the monohydrides of the alkali metals and the dihydrides of the alkaline-earth metals, with the exception of beryllium. BeH_2 appears to be a hydride with bridge type bonding rather than an ionic hydride. Highly polymerized molecules held together by hydrogen-bridge bonding is exhibited by boron hydrides and aluminum hydride. Based on the known structures of these hydrides, the ToF-SIMS hydride clusters such as $K[KH\,KHCO_3]_n^+$, the XPS peaks observed at $22.8\,eV$ and $38.8\,eV$, upfield NMR peaks assigned to hydride ion, and the shifted FTIR peaks, the present novel hydride compound of the $KH\,KHCO_3$ electrolytic cell sample may be a polymer, $[KH\,KHCO_3]_n$, with a structural formula which is similar to boron and aluminum hydrides. The reported novel compound

appeared polymeric in the concentrated electrolytic solution and in distilled water. $[KH\,KHCO_3]_n$ is extraordinarily stable in water; whereas, potassium hydride reacts violently with water.

As an example of the structures of this compound, the $K[KH\,KHCO_3]_n^+$ $m/z=(39+140n)$ series of fragment peaks is tentatively assigned to novel hydride bridged or linear potassium bicarbonate compounds having a general formula such as $[KHKHCO_3]_n$ $n=1,2,3....$ General structural formulas may be

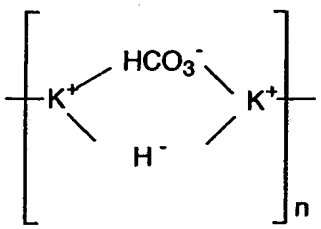

and

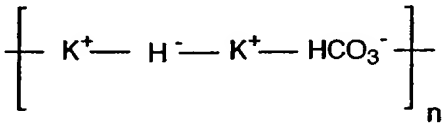

Liquid chromatography/ESIToFMS studies are in progress to support the polymer assignment.

The observation of inorganic hydride fragments such as $K[KH\,KHCO_3]^+$ in the positive ToF-SIMS spectra of samples isolated from the electrolyte following acidification indicates the stability of the novel potassium hydride potassium bicarbonate compound [10]. The electrolyte was acidified with HNO_3 to $pH=2$ and boiled to dryness to prepare samples to determine whether $KH\,KHCO_3$ was reactive under these conditions. Ordinarily no K_2CO_3 would be present, and the sample would be converted to KNO_3. Crystals were isolated by dissolving the dried crystals in water, concentrating the solution, and allowing crystals to precipitate. ToF-SIMS was performed on these crystals. The positive spectrum contained elements of the series of inorganic hydride clusters $\{K[KH\,KHCO_3]_n^+$ $m/z=(39+140n)$, $K_2OH[KH\,KHCO_3]_n^+$ $m/z=(95+140n)$, and $K_3O[KH\,KHCO_3]_n^+$ $m/z=(133+140n)\}$ that were observed in the positive ToF-SIMS spectrum of the $KH\,KHCO_3$ electrolytic cell sample as discussed in the ToF-SIMS Results Section and given in Figures 3-4 and Table 1. The presence of bicarbonate carbon ($C\,1s\cong 289.5\,eV$) was observed in the XPS of the sample from the HNO_3 acidified electrolyte. In addition, fragments

of compounds formed by the displacement of hydrogen carbonate by nitrate were observed [10]. A general structural formula for the reaction maybe

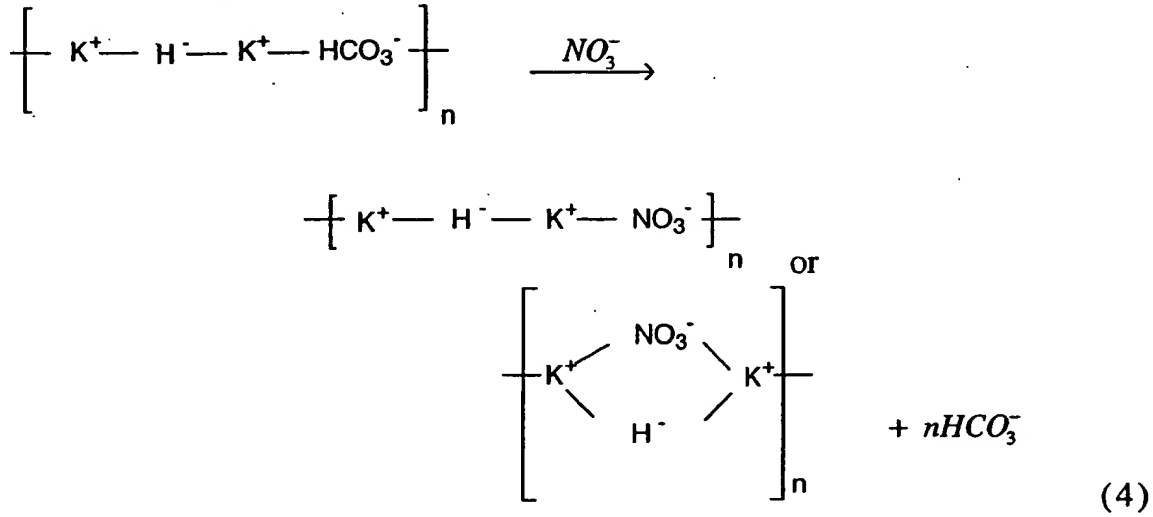

(4)

During acidification of the K_2CO_3 electrolyte the pH repetitively increased from 3 to 9 at which time additional acid was added with carbon dioxide release. The increase in pH (release of base by the titration reactant) was dependent on the temperature and concentration of the solution. A reaction consistent with this observation is the displacement reaction of NO_3^- for HCO_3^{2-} as given by Eq. (4).

KH was stable at elevated temperature (600 °C). The positive and negative ToF-SIMS of the *KH* electrolytic sample showed essentially K^+ and H^- only, respectively. Hydride ions with a binding energies of 22.8 *eV* and 69.2 *eV* have been observed by XPS of *KH*. The former hydride ion with a binding energy of 22.8 *eV* was observed by X-ray photoelectron spectroscopy (XPS) of the *KH KHCO*$_3$ electrolytic sample. These compounds appear polymeric in aqueous solution. *KH* was observed to be weakly ferromagnetic; whereas, *KH KHCO*$_3$ was diamagnetic. The magnetism of *KH* may be due to mixed oxidation states due to the presence of two hydride ions with a substantially reduced radii to permit spin correlation.

CONCLUSIONS

The ToF-SIMS, XPS, and NMR results confirm the identification of $KH\,KHCO_3$ and KH with a new states of hydride ions. The chemical structure and properties of these compounds having hydride ions with high binding energies are indicative of a new field of hydride chemistry. The novel hydride ions may combine with other cations such as other alkali cations and alkaline earth, rare earth, and transition element cations. Thousands of novel compounds may be synthesized with extraordinary properties relative to the corresponding compounds having ordinary hydride ions. These novel compounds may have a breath of applications. For example, a high voltage battery (Eqs. (1-3)) according to the hydride binding energies of $22.8\,eV$ and $69.2\,eV$ observed by XPS may be possible having projected specifications that surpass those of the internal combustion engine.

ACKNOWLEDGMENTS

Special thanks to Bala Dhandapani for work on the Raman, FTIR, and XRD studies. Special thanks to Jiliang He for obtaining the MAS NMR spectrum of potassium hydride. Special thanks to Bala Dhandapani and Jiliang He for helpful comments upon review of the manuscript.

APPENDIX

A novel hydride ion having extraordinary chemical properties given by Mills [10] is predicted to form by the reaction of an electron with a hydrino (Eq. (6)), a hydrogen atom having a binding energy given by

$$Binding\ Energy = \frac{13.6\ eV}{\left(\frac{1}{p}\right)^2} \tag{5}$$

where p is an integer greater than 1, designated as $H\left[\frac{a_H}{p}\right]$ where a_H is the radius of the hydrogen atom. The resulting hydride ion is referred to as a hydrino hydride ion, designated as $H^-(1/p)$.

$$H\left[\frac{a_H}{p}\right]+e^- \rightarrow H^-(1/p) \tag{6}$$

The hydrino hydride ion is distinguished from an ordinary hydride ion having a binding energy of 0.8 eV. The latter is hereafter referred to as "ordinary hydride ion". The hydrino hydride ion is predicted [10] to comprise a hydrogen nucleus and two indistinguishable electrons at a binding energy according to the following formula:

$$Binding\ Energy = \frac{\hbar^2\sqrt{s(s+1)}}{8\mu_e a_0^2\left[\frac{1+\sqrt{s(s+1)}}{p}\right]^2} - \frac{\pi\mu_0 e^2\hbar^2}{m_e^2 a_0^3}\left(1+\frac{2^2}{\left[\frac{1+\sqrt{s(s+1)}}{p}\right]^3}\right) \tag{7}$$

where p is an integer greater than one, $s=1/2$, π is pi, $\hbar$ is Planck's constant bar, μ_o is the permeability of vacuum, m_e is the mass of the electron, μ_e is the reduced electron mass, a_o is the Bohr radius, and e is the elementary charge. The ionic radius is

$$r_1 = \frac{a_0}{p}\left(1+\sqrt{s(s+1)}\right);\ s=\frac{1}{2} \tag{8}$$

From Eq. (8), the radius of the hydrino hydride ion $H^-(1/p);\ p=\text{integer}$ is $\frac{1}{p}$ that of ordinary hydride ion, $H^-(1/1)$. The XPS peaks of KH $KHCO_3$ centered at $22.8\,eV$ and $38.8\,eV$ and the XPS peaks of KH centered at $19.5\,eV$ and $36.0\,eV$ are assigned to shifted $K\,3s$ and $K\,3p$. The anion does not correspond to any other primary element peaks; thus, it may correspond to the $H^-(n=1/6)\,E_b=22.8\,eV$ hydride ion predicted by Mills [10] where E_b is the predicted binding energy. The XPS peak of KH centered at $68.0\,eV$ is assigned to $H^-(n=1/14)\,E_b=69.2\,eV$

Hydrinos are predicted to form by reacting an ordinary hydrogen atom with a catalyst having a net enthalpy of reaction of about

$$m\cdot 27.21\,eV \tag{9}$$

where m is an integer [10]. This catalysis releases energy from the hydrogen atom with a commensurate decrease in size of the hydrogen atom, $r_n = na_H$. For example, the catalysis of $H(n=1)$ to $H(n=1/2)$ releases $40.8\,eV$, and the hydrogen radius decreases from a_H to $\frac{1}{2}a_H$. One such catalytic system involves potassium. The second ionization energy of potassium is $31.63\,eV$; and K^+ releases $4.34\,eV$ when it is reduced to K.

The combination of reactions K^+ to K^{2+} and K^+ to K, then, has a net enthalpy of reaction of $27.28\,eV$, which is equivalent to $m=1$ in Eq. (9).

$$27.28\,eV + K^+ + K^+ + H\left[\frac{a_H}{p}\right] \rightarrow K + K^{2+} + H\left[\frac{a_H}{(p+1)}\right] + [(p+1)^2 - p^2]\,X\,13.6\,eV \qquad (10)$$

$$K + K^{2+} \rightarrow K^+ + K^+ + 27.28\,eV \qquad (11)$$

The overall reaction is

$$H\left[\frac{a_H}{p}\right] \rightarrow H\left[\frac{a_H}{(p+1)}\right] + [(p+1)^2 - p^2]\,X\,13.6\,eV \qquad (12)$$

The energy given off during catalysis is much greater than the energy lost to the catalyst. The energy released is large as compared to conventional chemical reactions. For example, when hydrogen and oxygen gases undergo combustion to form water

$$H_2(g) + \frac{1}{2}O_2(g) \rightarrow H_2O(l) \qquad (13)$$

the known formation enthalpy of water is $\Delta H_f = -286\,kJ/mole$ or 1.48 eV per hydrogen atom. By contrast, each ordinary hydrogen atom ($n=1$) catalysis releases a net of $40.8\,eV$.

Calorimetry of pulsed current and continuous electrolysis of aqueous potassium carbonate at a nickel cathode were performed at Thermacore, Inc., Lancaster, PA [7]. This cell had produced an enthalpy of formation of novel hydride compounds of $1.6\,X\,10^9\,J$ that exceeded the total input enthalpy given by the product of the electrolysis voltage and current over time by a factor greater than 8. The exothermic reactions Eq. (10-12), Eq. (6) and the enthalpy of formation of $KH\,KHCO_3$ could explain the observation of excess enthalpy.

Calorimetry of pulsed current electrolysis of aqueous potassium carbonate at a nickel cathode was performed at Idaho National Engineering Laboratory. The cell was wrapped in a one-inch layer of urethane foam insulation about the cylindrical surface. The cell was operated in a pulsed power mode. A current of 10 amperes was passed through the cell for 0.2 seconds followed by 0.8 seconds of zero current for the current cycle. The cell voltage was about 2.4 volts, for an average input power of 4.8 W. The electrolysis power average was 1.84 W, and the stirrer power was measured to be 0.3 W. Thus, the total average net input power was 2.14 W. The cell was operated at various resistance heater settings, and the temperature difference between the cell and the

ambient as well as the heater power were measured. The results of the excess power as a function of cell temperature with the cell operating in the pulsed power mode at 1 Hz with a cell voltage of 2.4 volts, a peak current of 10 amperes, and a duty cycle of 20 % showed that the excess power is temperature dependent for pulsed power operation, and the maximum excess power was 18 W for an input electrolysis joule heating power of 2.14 W. Thus, the ratio of excess power to input electrolysis joule heating power was 850 % [17]. The exothermic reactions Eq. (10-12), Eq. (6) and the enthalpy of formation of *KH* could explain the observation of excess enthalpy.

REFERENCES

1. I. Uehara, T. Sakai, H. Ishikawa, J. Alloy Comp., 253/254, (1997), pp. 635-641.
2. J. Glanz, "Check the Tires and Charge Her Up", New Scientist, April 15, (1995) pp. 32-35.
3. D. Mulholland, Defense News, "Powering the Future Military", March 8, 1999, pp. 1&34.
4. S. M. Aceves, G. D. Berry, and G. D. Rambach, Int. J. Hydrogen Energy, Vol. 23, No. 7, (1998), pp. 583-591.
5. J. Ball, The Wall Street Journal, "Auto Makers Are Racing to Market "Green" Cars Powered by Fuel Cells", March 15, 1999, p. 1.
6. "Advanced Automotive Technology: Visions of a Super-Efficient Family Car", National Technical Information Service, US Department of Commerce, US Office of Technology Assessment, Washington, DC PB96-109202, September 1995.
7. R. Mills, W. Good, and R. Shaubach, Fusion Technol. 25, 103 (1994).
8. Microsc. Microanal. Microstruct., Vol. 3, 1, (1992).
9. For recent specifications see PHI Trift II, ToF-SIMS Technical Brochure, (1999), Eden Prairie, MN 55344.
10. R. Mills, *The Grand Unified Theory of Classical Quantum Mechanics*, January 1999 Edition, BlackLight Power, Inc., Cranbury, New Jersey, Distributed by Amazon.com.
11. *Practical Surface Analysis*, 2nd Edition, Volume 2, Ion and Neutral Spectroscopy, D. Briggs, M. P. Seah (Editors), Wiley & Sons, New York, (1992).
12. C. D. Wagner, W. M. Riggs, L. E. Davis, J. F. Moulder, G. E. Mulilenberg (Editor), *Handbook of X-ray Photoelectron Spectroscopy*, Perkin-Elmer Corp., Eden Prairie, Minnesota, (1997).
13. D. Lin-Vien, N. B. Colthup, W. G. Fateley, J. G. Grassellic, *The Handbook of Infrared and Raman Characteristic Frequencies of Organic Molecules*, Academic Press, Inc., (1991).
14. R. A. Nyquist and R. O. Kagel, (Editors), *Infrared Spectra of Inorganic Compounds*, Academic Press, New York, (1971).
15. M. H. Brooker, J. B. Bates, *Spectrochimica Acta*, Vol. 30A, (1994), pp. 2211-2220.

16. R. Mills, B. Dhandapani, M. Nansteel, J. He, "Synthesis and Characterization of Novel Hydride Compounds", Int. J. of Hydrogen Energy, submitted.
17. Jacox, M. G., Watts, K. D., "The Search for Excess Heat in the Mills Electrolytic Cell", Idaho National Engineering Laboratory, EG&G Idaho, Inc., Idaho Falls, Idaho, 83415, January 7, 1993.

Table 1. The respective hydride compounds and mass assignments (m/z) of the positive ToF-SIMS of the $KH\,KHCO_3$ electrolytic cell sample.

Hydrino Hydride Compound or Fragment	Nominal Mass m/z	Observed m/z	Calculated m/z	Difference Between Observed and Calculated m/z
KH	40	39.97	39.971535	0.0015
K_2H	79	78.940	78.935245	0.004
$(KH)_2$	80	79.942	79.94307	0.001
$KHKOH_2$	97	96.945	96.945805	0.0008
$KH_2(KH)_2$	121	120.925	120.92243	0.003
$KH\,KHCO_2$	124	123.925	123.93289	0.008
KH_2KHO_4	145	144.92	144.930535	0.010
$K(KOH)_2$	151	150.90	150.8966	0.003
$KH(KOH)_2$	152	151.90	151.904425	0.004
$KH_2(KOH)_2$	153	152.90	152.91225	0.012
$K[KH\ KHCO_3]$	179	178.89	178.8915	0.001
$KCO(KH)_3$	187	186.87	186.873225	0.003
$K_2OHKHKOH$	191	190.87	190.868135	0.002
$KH_2KOHKHKOH$	193	192.89	192.883785	0.006
$K_3O(H_2O)_4$	205	204.92	204.92828	0.008
$K_2OH[KH\,KHCO_3]$	235	234.86	234.857955	0.002
$K[H_2CO_4\,KH\,KHCO_3]$	257	256.89	256.8868	0.003
$K_3O[KH\,KHCO_3]$	273	272.81	272.81384	0.004
$[KH_2CO_3]_3$	303	302.88	302.89227	0.012
$K[KH\ KHCO_3K_2CO_3]$	317	316.80	316.80366	0.004
$K[KH\ KHCO_3]_2$	319	318.82	318.81931	0.001
$KH_2[KH\,KOH]_3$	329	328.80	328.7933	0.007
$KOH_2[KH\,KHCO_3]_2$	337	336.81	336.82987	0.020
$KH\,KO_2$ $[KH\,KHCO_3][KHCO_3]$	351	350.81	350.80913	0.001
$KKHK_2CO_3$ $[KH\,KHCO_3]$	357	356.77	356.775195	0.005

$KKH[KH\ KHCO_3]_2$	359	358.78	358.790845	0.011
$K_2OH[KH\ KHCO_3]_2$	375	374.78	374.785755	0.005
$K_2OH[KHKOH]_2$ $[KHCO_3]$	387	386.75	386.76238	0.012
$KKH_3KH_5[KH\ KHCO_3]_2$	405	404.79	404.80933	0.019
$K_3O[K_2CO_3]$ $[KH\ KHCO_3]$ or $K[KH\ KOH(K_2CO_3)_2]$	411	410.75	410.72599	0.024
$K_3O[KH\ KHCO_3]_2$	413	412.74	412.74164	0.002
$K\begin{bmatrix} KH\ KOH \\ (KH\ KHCO_3)_2 \end{bmatrix}$	415	414.74	414.75729	0.017
KH_2OKHCO_3 $[KH\ KHCO_3]_2$	437	436.81	436.786135	0.024
$KKHKCO_2[KH\ KHCO_3]_2$	442	441.74	441.744375	0.004
$K[KH\ \ KHCO_3]_3$	459	458.72	458.74711	0.027
$H[KH\ KOH]_2[K_2CO_3]_2$ or $K_4O_2H[KH\ KHCO_3]_2$	469	468.70	468.708085	0.008
$K[K_2CO_3][KHCO_3]_3$	477	476.72	476.744655	0.025
$K_2OH[KH\ KHCO_3]_3$	515	514.72	514.713555	0.006
$K_3O[KH\ KHCO_3]_3$	553	552.67	552.66944	0.001
$K[KH\ \ KHCO_3]_4$	599	598.65	598.67491	0.025
$K_2OH[KH\ KHCO_3]_4$	655	654.65	654.641355	0.009
$K_3O[KH\ KHCO_3]_4$	693	692.60	692.59724	0.003
$K[KH\ \ KHCO_3]_5$	739	738.65	738.60271	0.047
$K_3O[KH\ KHCO_3]_5$	833	832.50	832.52504	0.025
$K[KH\ \ KHCO_3]_6$	879	878.50	878.53051	0.031
$K_3O[KH\ KHCO_3]_6$	973	972.50	972.45284	0.047

Table 2. The binding energies of XPS peaks of K_2CO_3 and the $KH\,KHCO_3$ electrolytic cell sample.

XPS #	$C\,1s$ (eV)	$O\,1s$ (eV)	$K\,3p$ (eV)	$K\,3s$ (eV)	$K\,2p_3$ (eV)	$K\,2p_1$ (eV)	$K\,2s$ (eV)
K_2CO_3	288.4	532.0	18	34	292.4	295.2	376.7
$KH\,KHCO_3$	288.5	530.4	16.2	32.1	291.5	293.7	376.6
Electrolytic		537.5	22.8	38.8	298.5	300.4	382.6
Cell		547.8					
Sample							
Min	280.5	529			292		
Max	293	535			293.2		

Table 3. The NMR peaks of the $KH\,KHCO_3$ electrolytic cell sample with their assignments.

Peak at Shift (ppm)	Assignment
+34.54	side band of +17.163 peak
+22.27	side band of +5.066 peak
+17.163	$KH\,KHCO_3$
+10.91	$KH\,KHCO_3$
+8.456	$KH\,KHCO_3$
+7.50	$KH\,KHCO_3$
+5.066	H_2O
+1.830	$KH\,KHCO_3$
-0.59	side band of +17.163 peak
-12.05	$KH\,KHCO_3$ [a]
-15.45	$KH\,KHCO_3$

[a] small shoulder is observed on the -12.05 peak which is the side band of the +5.066 peak

Figure 1. The positive ToF-SIMS spectrum ($m/e = 0-200$) of $KHCO_3$ (99.99%) where HC = hydrocarbon.

Figure 2. The positive ToF-SIMS spectrum ($m/e = 200-1000$) of $KHCO_3$ (99.99%) where HC = hydrocarbon.

Figure 3. The positive ToF-SIMS spectrum ($m/e = 0-200$) of the $KH\,KHCO_3$ electrolytic cell sample where HC = hydrocarbon.

Figure 4. The positive ToF-SIMS spectrum ($m/e = 200-1000$) of the $KH\,KHCO_3$ electrolytic cell sample where HC = hydrocarbon.

Figure 5. The negative ToF-SIMS spectrum ($m/e = 0-50$) of the $KHCO_3$ (99.99%) sample.

Figure 6. The negative ToF-SIMS spectrum ($m/e = 0-30$) of the $KH\,KHCO_3$ electrolytic cell sample.

Figure 7. The positive ToF-SIMS spectrum of the *KH* electrolytic cell sample.

Figure 8. The negative ToF-SIMS spectrum of the *KH* electrolytic cell sample.

Figure 9. The 0 to 80 eV binding energy region of a high resolution XPS spectrum of the $KH\,KHCO_3$ electrolytic cell sample.

Figure 10. The XPS survey spectrum of the $KH\,KHCO_3$ electrolytic cell sample with the primary elements identified.

Figure 11. The XPS survey scan of the *KH* electrolytic cell sample.

Figure 12. The 0-80 eV binding energy region of a high resolution XPS spectrum of the *KH* electrolytic cell sample.

Figure 13. The magic angle spinning proton NMR spectrum of the $KH\,KHCO_3$ electrolytic cell sample.

Figure 14. The overlap FTIR spectrum of the $KH\,KHCO_3$ electrolytic cell sample and the FTIR spectrum of the reference potassium carbonate.

Fig 1

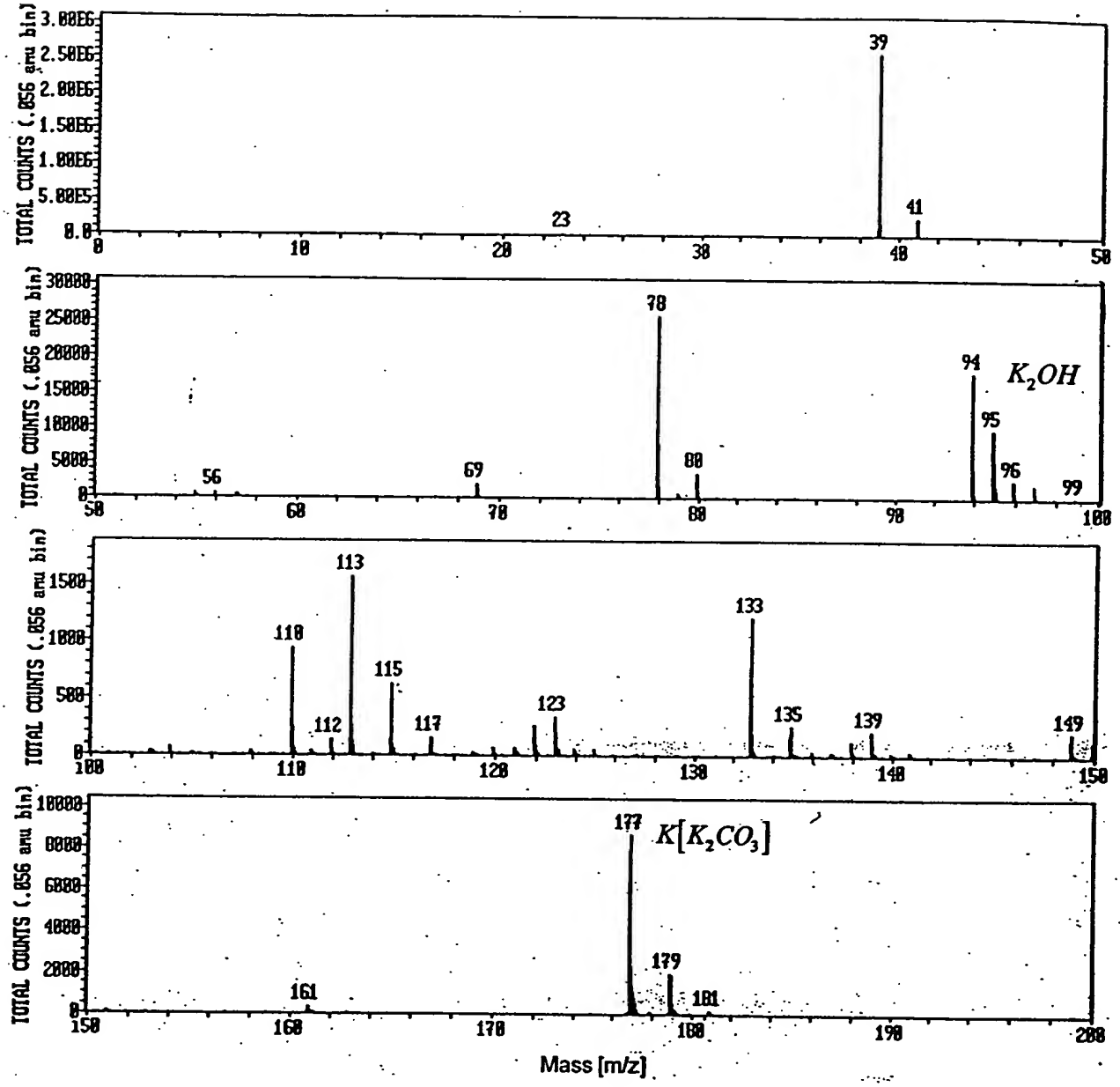
TOTAL COUNTS (.856 amu bin)
3.00E6
2.50E6
2.00E6
1.50E6
1.00E6
5.00E5
0.0
39
23
41
0
10
20
30
40
50
30000
25000
20000
15000
10000
5000
0
78
94
K_2OH
95
56
69
80
96
99
50
60
70
80
90
100
1500
1000
500
0
113
110
115
133
112
117
123
135
139
149
100
110
120
130
140
150
10000
8000
6000
4000
2000
0
177
$K[K_2CO_3]$
179
161
181
150
160
170
180
190
200
Mass [m/z]

F.3.2

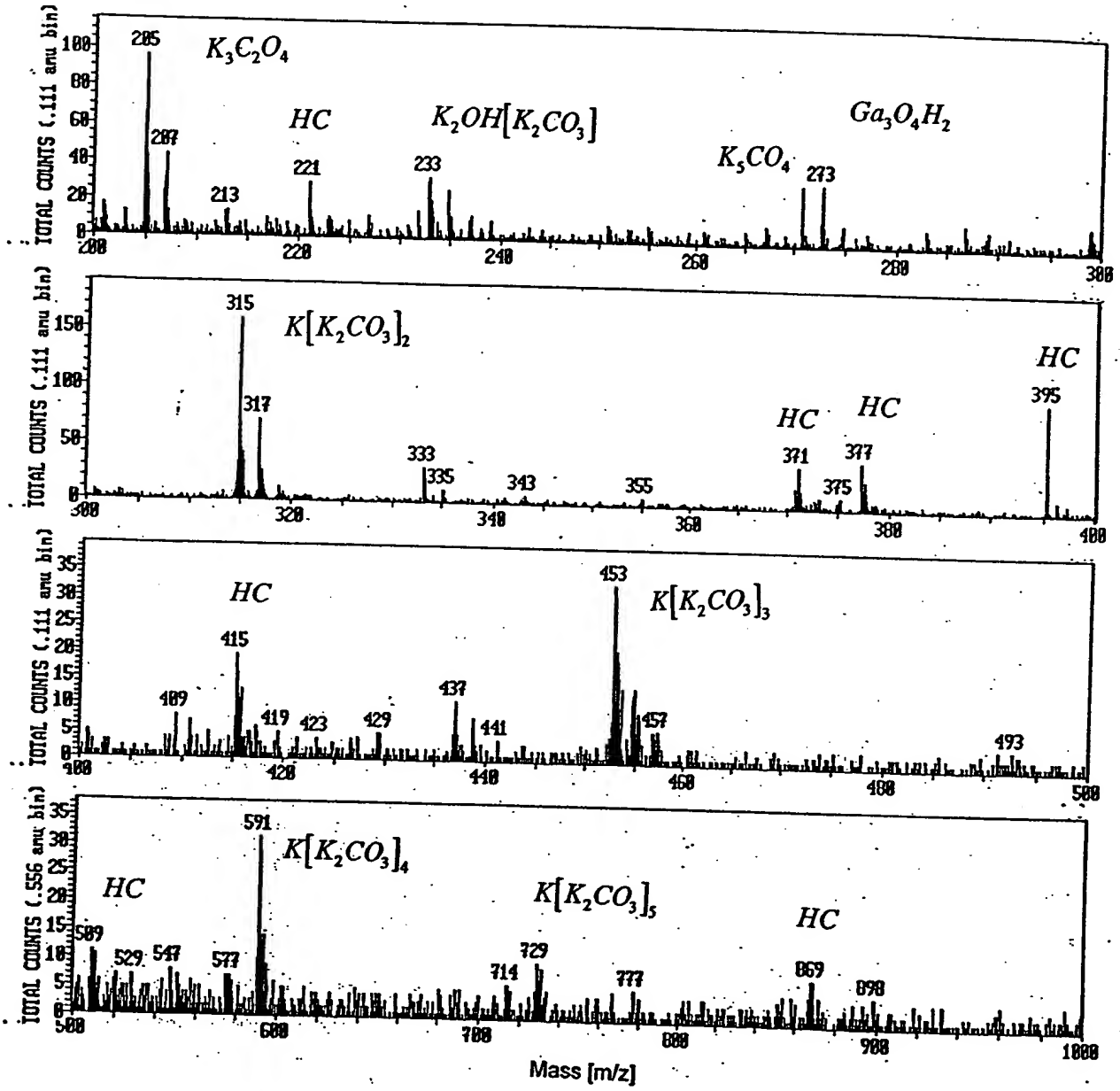
TOTAL COUNTS (.111 amu bin)
285
$K_3C_2O_4$
287
213
HC
221
$K_2OH[K_2CO_3]$
233
K_5CO_4
273
$Ga_3O_4H_2$
TOTAL COUNTS (.111 amu bin)
315
$K[K_2CO_3]_2$
317
333
335
343
355
HC
371
HC
377
375
HC
395
TOTAL COUNTS (.111 amu bin)
HC
415
409
419
423
429
437
441
453
$K[K_2CO_3]_3$
457
493
TOTAL COUNTS (.556 amu bin)
591
$K[K_2CO_3]_4$
HC
589
529
547
577
$K[K_2CO_3]_5$
714
729
777
HC
869
898
Mass [m/z]

Fig 3

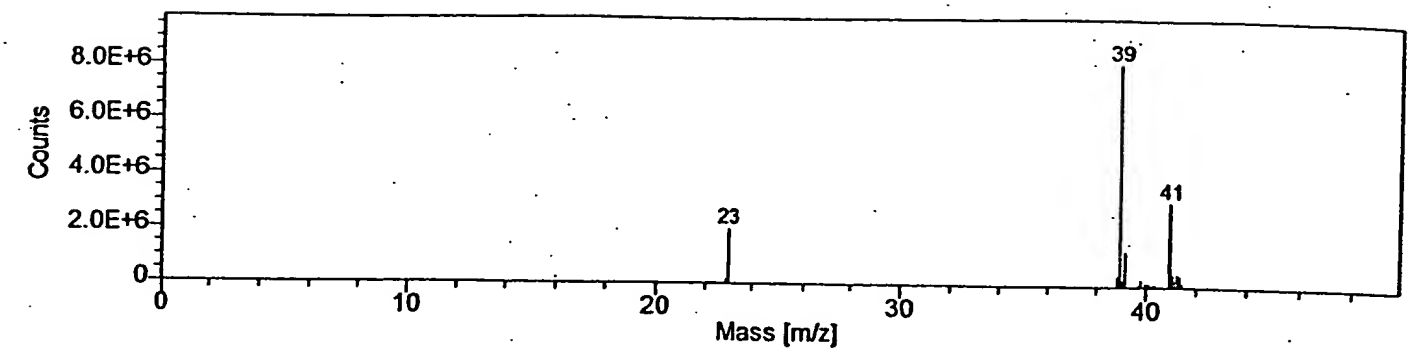
Counts
8.0E+6
6.0E+6
4.0E+6
2.0E+6
0
0
10
20
30
40
Mass [m/z]
39
41
23

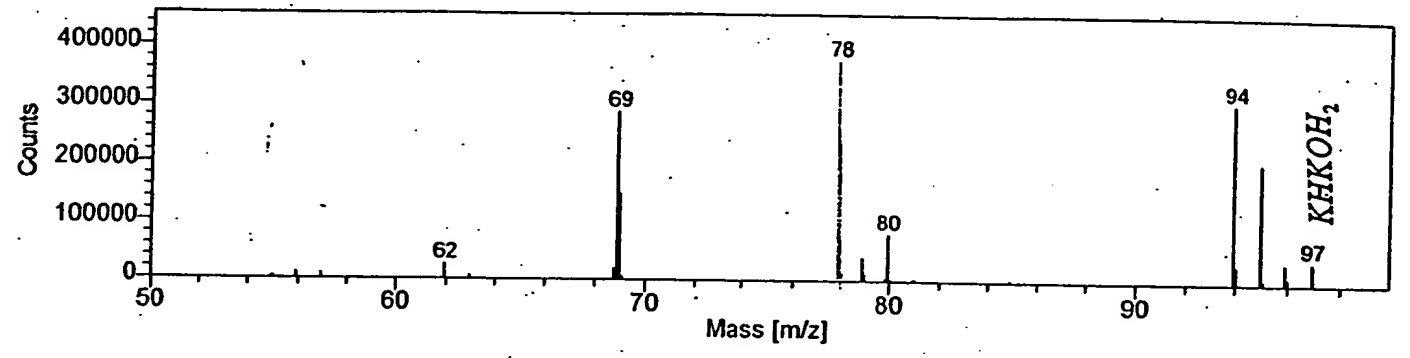
Counts
400000
300000
200000
100000
0
50
60
70
80
90
Mass [m/z]
78
69
94
80
62
97
KHKOH2

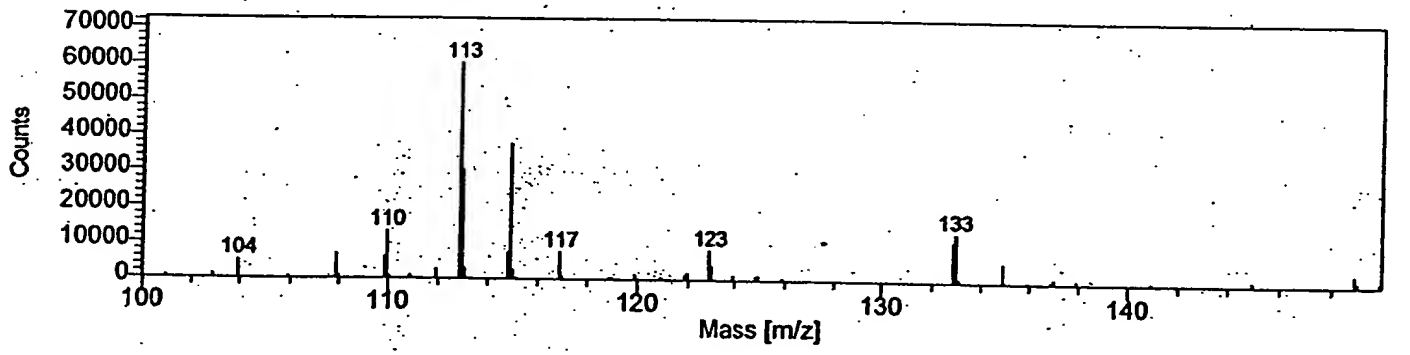
Counts
70000
60000
50000
40000
30000
20000
10000
0
100
110
120
130
140
Mass [m/z]
113
110
104
117
123
133

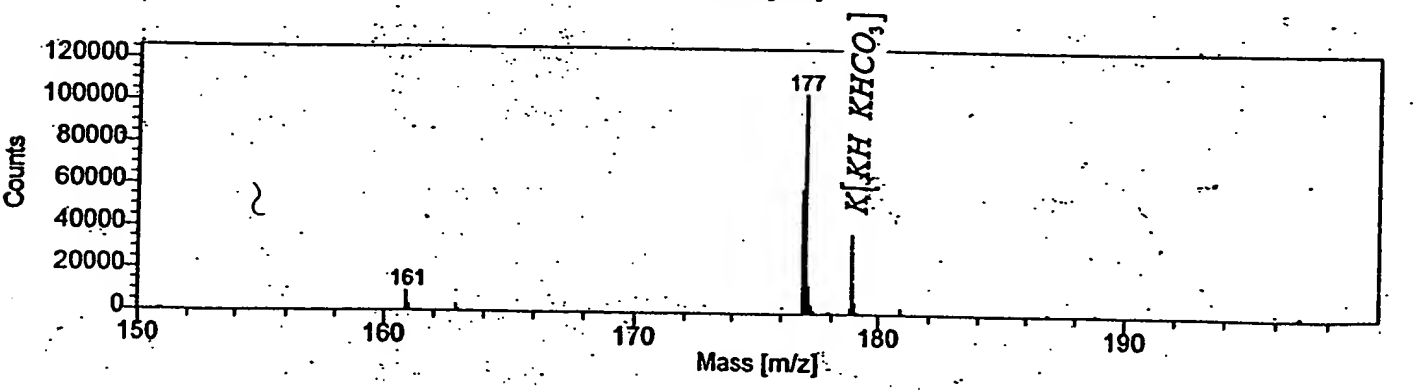
Counts
120000
100000
80000
60000
40000
20000
0
150
160
170
180
190
Mass [m/z]
177
161
K[KH KHCO3]

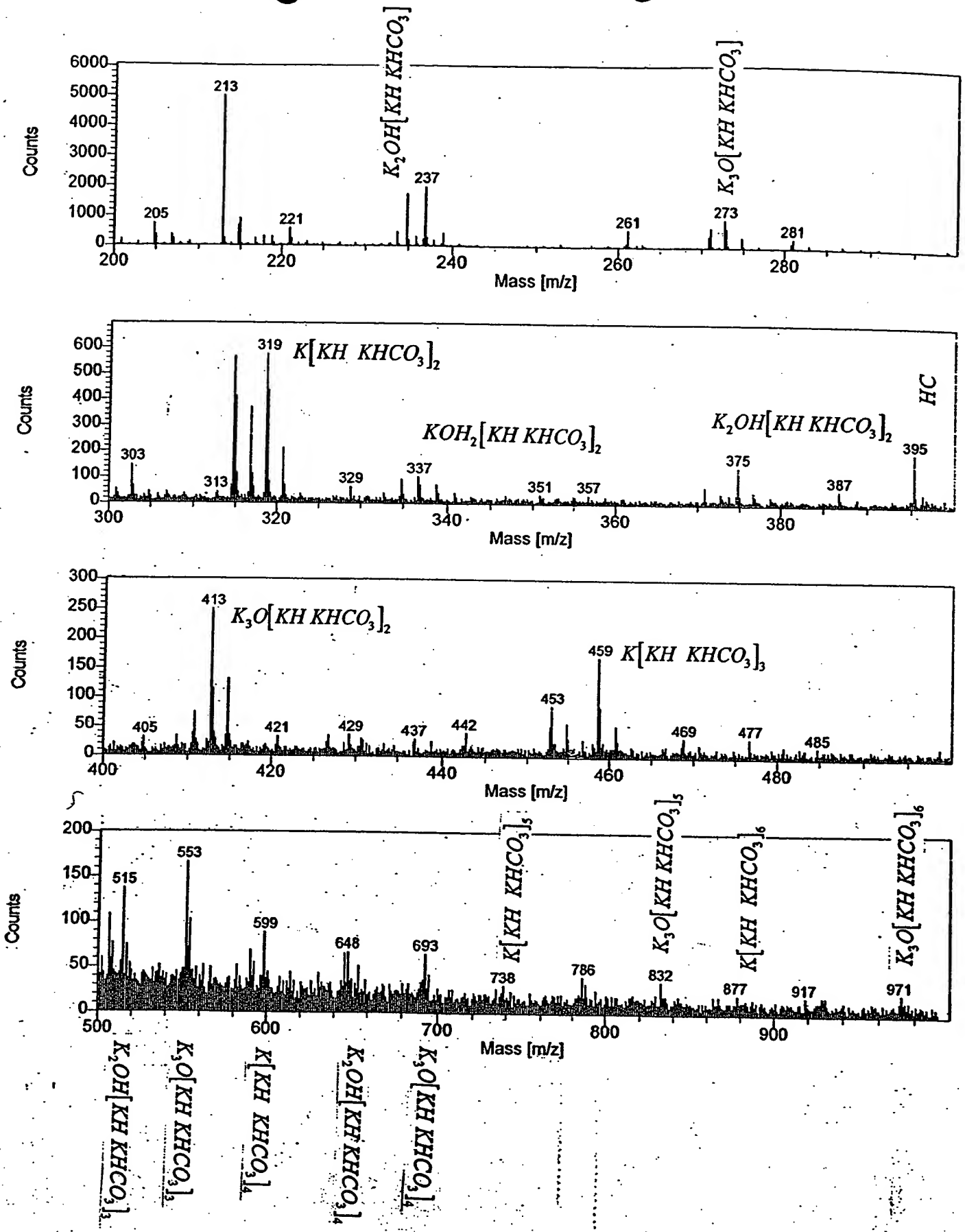
Counts
Mass [m/z]
213
205
221
237
261
273
281
$K_2OH[KH\ KHCO_3]$
$K_3O[KH\ KHCO_3]$
319
303
313
329
337
351
357
375
387
395
$K[KH\ KHCO_3]_2$
$KOH_2[KH\ KHCO_3]_2$
$K_2OH[KH\ KHCO_3]_2$
413
405
421
429
437
442
453
459
469
477
485
$K_3O[KH\ KHCO_3]_2$
$K[KH\ KHCO_3]_3$
515
553
599
648
693
738
786
832
877
917
971
$K[KH\ KHCO_3]_{15}$
$K_3O[KH\ KHCO_3]_{15}$
$K[KH\ KHCO_3]_{16}$
$K_3O[KH\ KHCO_3]_{16}$
$K_2OH[KH\ KHCO_3]_{13}$
$K_3O[KH\ KHCO_3]_{13}$
$K[KH\ KHCO_3]_{14}$
$K_2OH[KH\ KHCO_3]_{14}$
$K_3O[KH\ KHCO_3]_{14}$

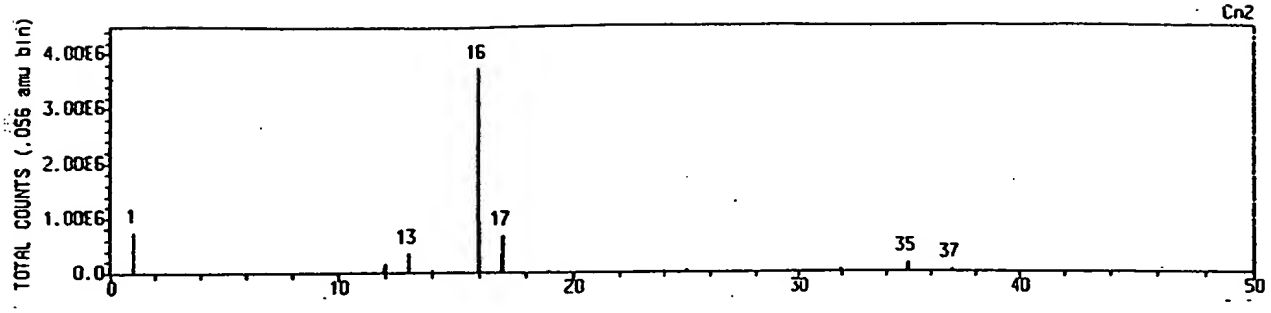
Cn2
TOTAL COUNTS (.056 amu bin)
4.00E6
3.00E6
2.00E6
1.00E6
0.0
1
13
16
17
35
37
0
10
20
30
40
50

Fig. 5

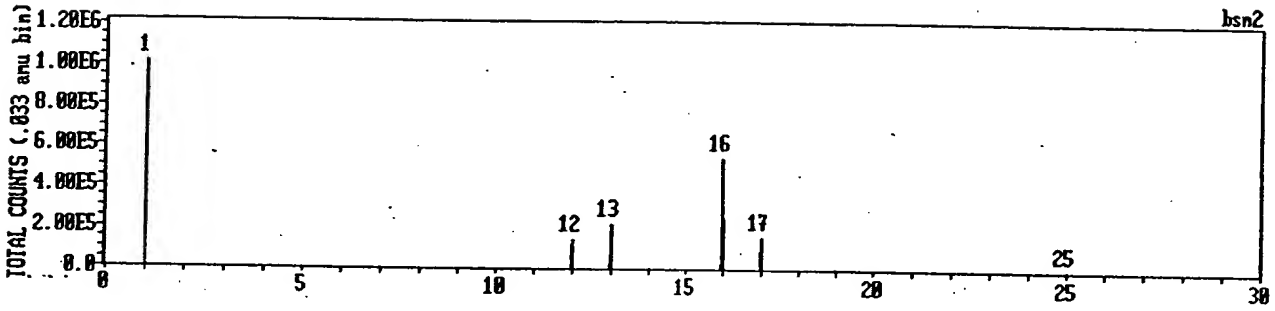
TOTAL COUNTS (.033 amu bin)
1.20E6
1.00E6
8.00E5
6.00E5
4.00E5
2.00E5
0.0
0
5
10
15
20
25
30
bsn2
1
12
13
16
17
25

Fig. 6

BLACKLIGHT POWER, INC.
ANALYTICAL SERVICES GROUP
SURFACE ANALYSIS LABORATORY
T:609-490-1090 F:609-490-1066

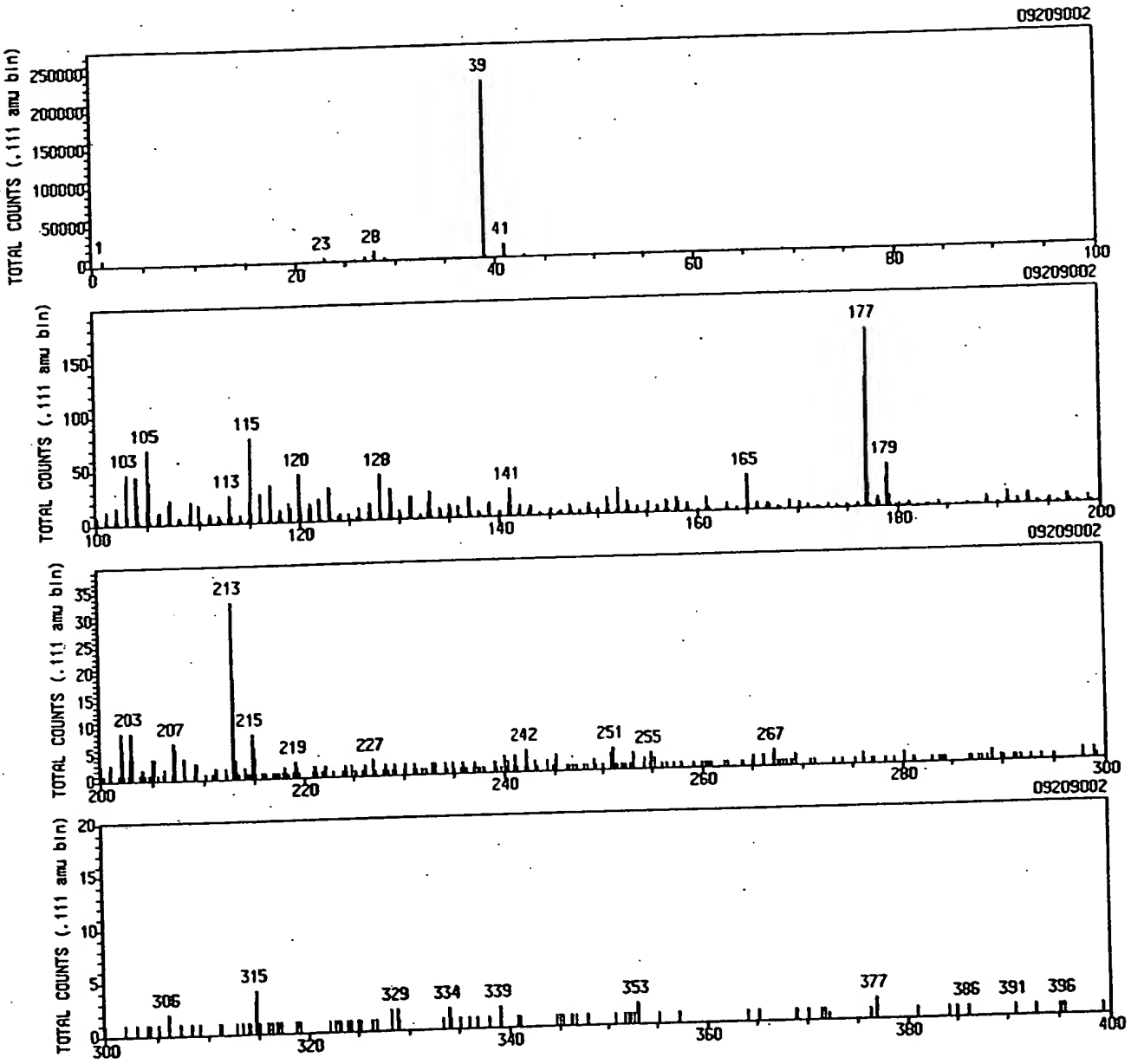

FILE NAME: 09209002 DATE : 20 Sep 99 16:53 ACQUISITION TIME: 5.0 MIN. SPECTRUM INTEGRAL : 319972
990917rm,+, 7ns, e-on, buch805, 5 minAqt, non-sput,(another spot;
+ IONS PRIMARY GUN: LMIG TIME RECORDER: Multi-Stop TDC X-Y SOURCE: RAE TIME PER CHANNEL: 138 ps
DATA SET: 1 Spectra; 0 Image(s) RASTER SIZE: 61µm RASTER TYPE: Full NI FlyBack

990917an
K+Hy
INEL

Fig. 7

FIGURE____

BLACKLIGHT POWER, INC.
ANALYTICAL SERVICES GROUP
SURFACE ANALYSIS LABORATORY
T:609-490-1090 F:609-490-1066

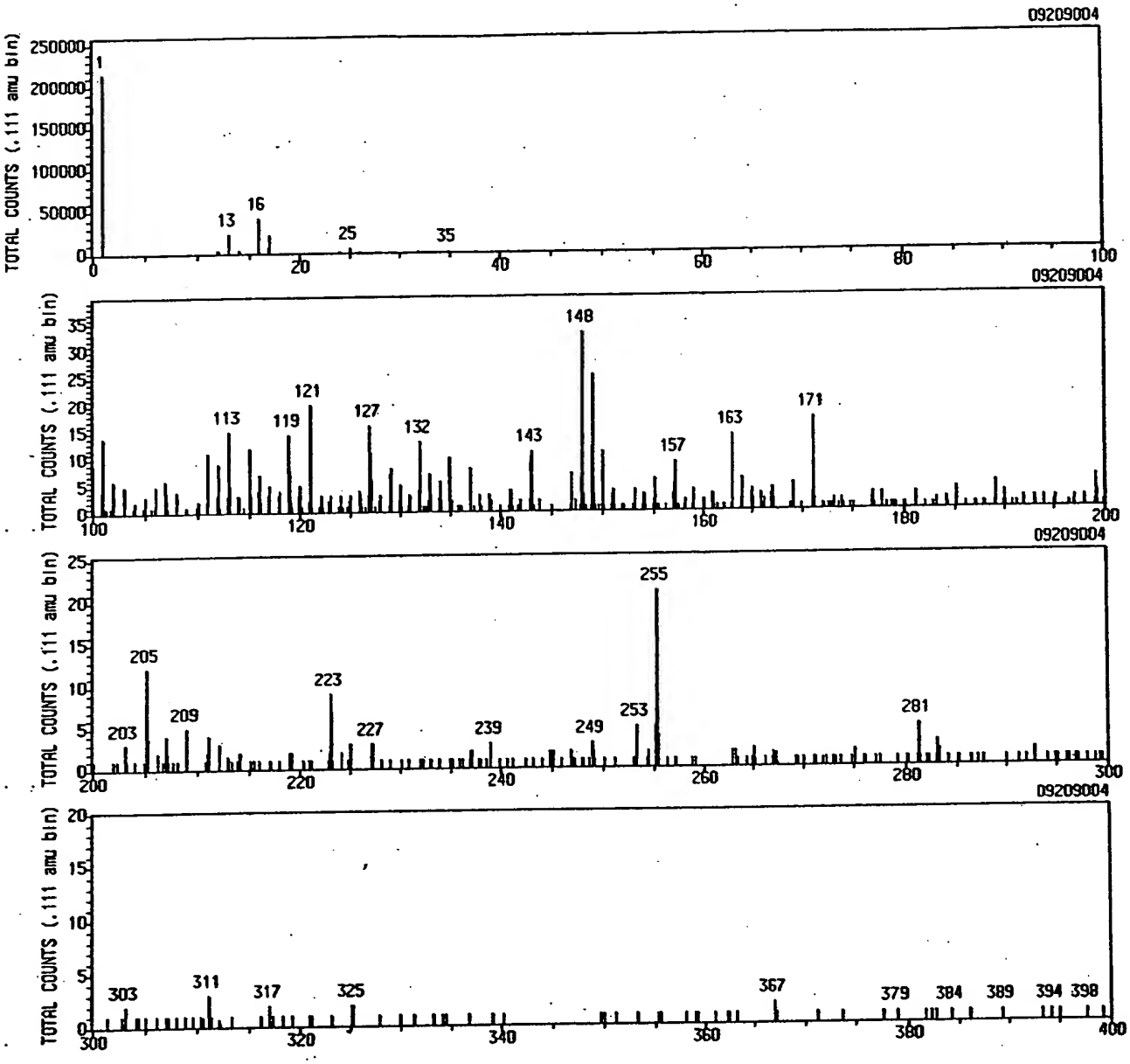

FILE NAME: 09209004 DATE : 20 Sep 99 17:10 ACQUISITION TIME: 5.0 MIN. SPECTRUM INTEGRAL : 343853
990917rm,-, 7ns, e-on, buch805, 5 minAqt, 30s-sput,;
- IONS PRIMARY GUN: LMIG TIME RECORDER: Multi-Stop TDC X-Y SOURCE: RAE TIME PER CHANNEL: 138 ps
DATA SET: 1 Spectra; 0 Image(s) RASTER SIZE: 61µm RASTER TYPE: Full NI FlyBack

990917rm
Ion My
Image

Fig. 8

FIGURE____

Fig 9

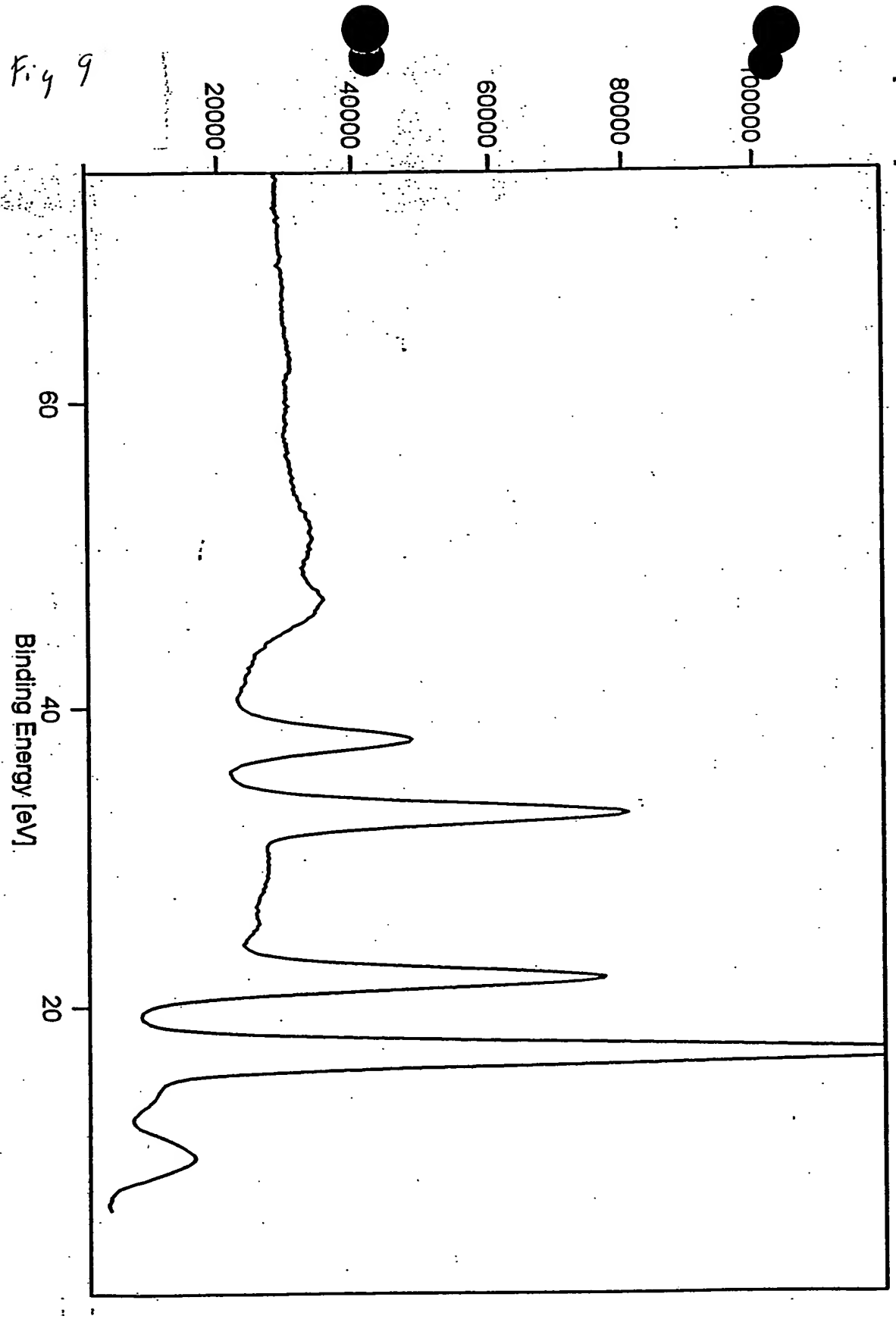
[Counts]
20000
40000
60000
80000
100000
Binding Energy [eV]
60
40
20

Fig. 10

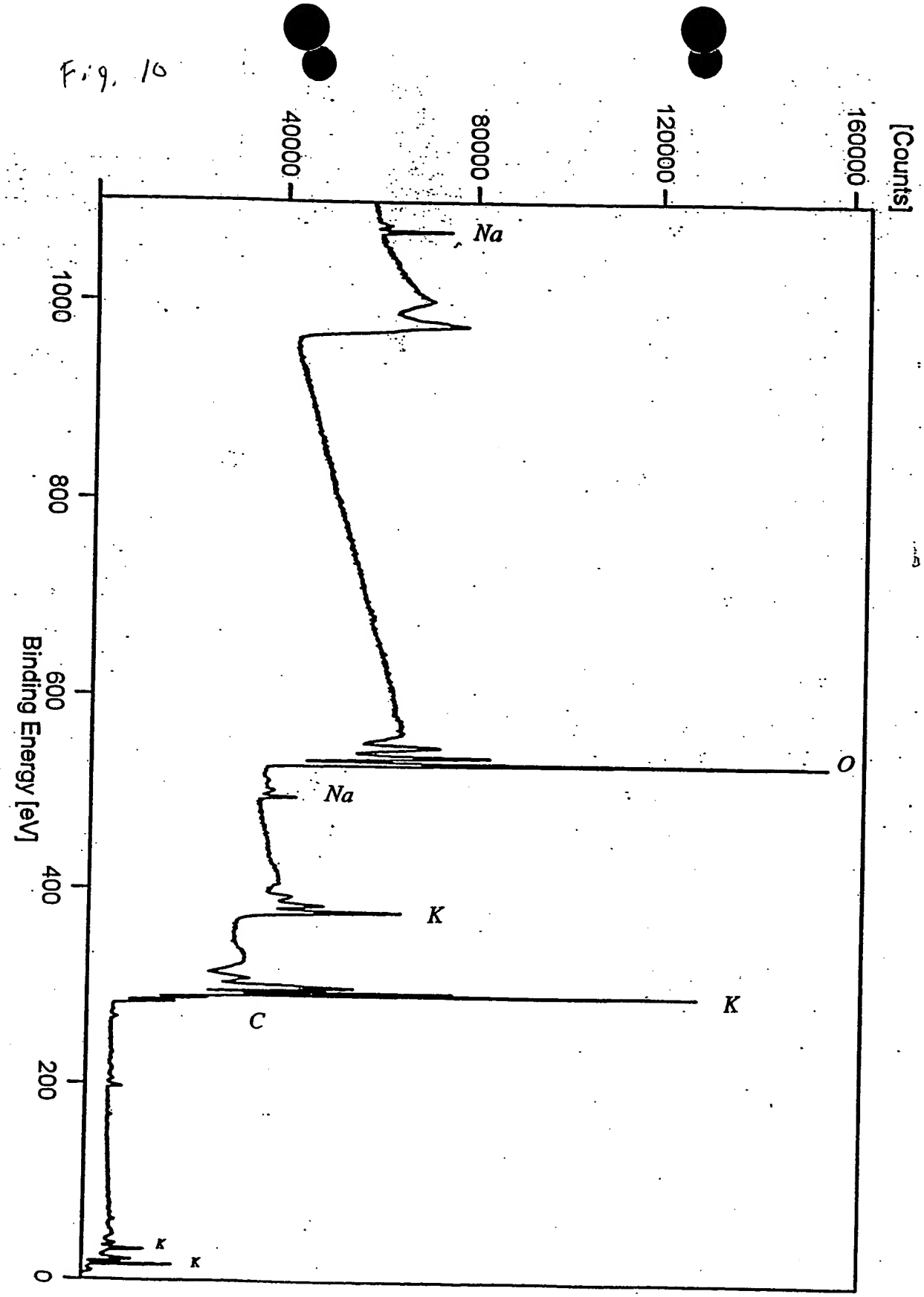
40000
80000
120000
160000
[Counts]
1000
800
600
400
200
0
Binding Energy [eV]
Na
O
Na
K
C
K
K
K

917 Rm
Fig. 11

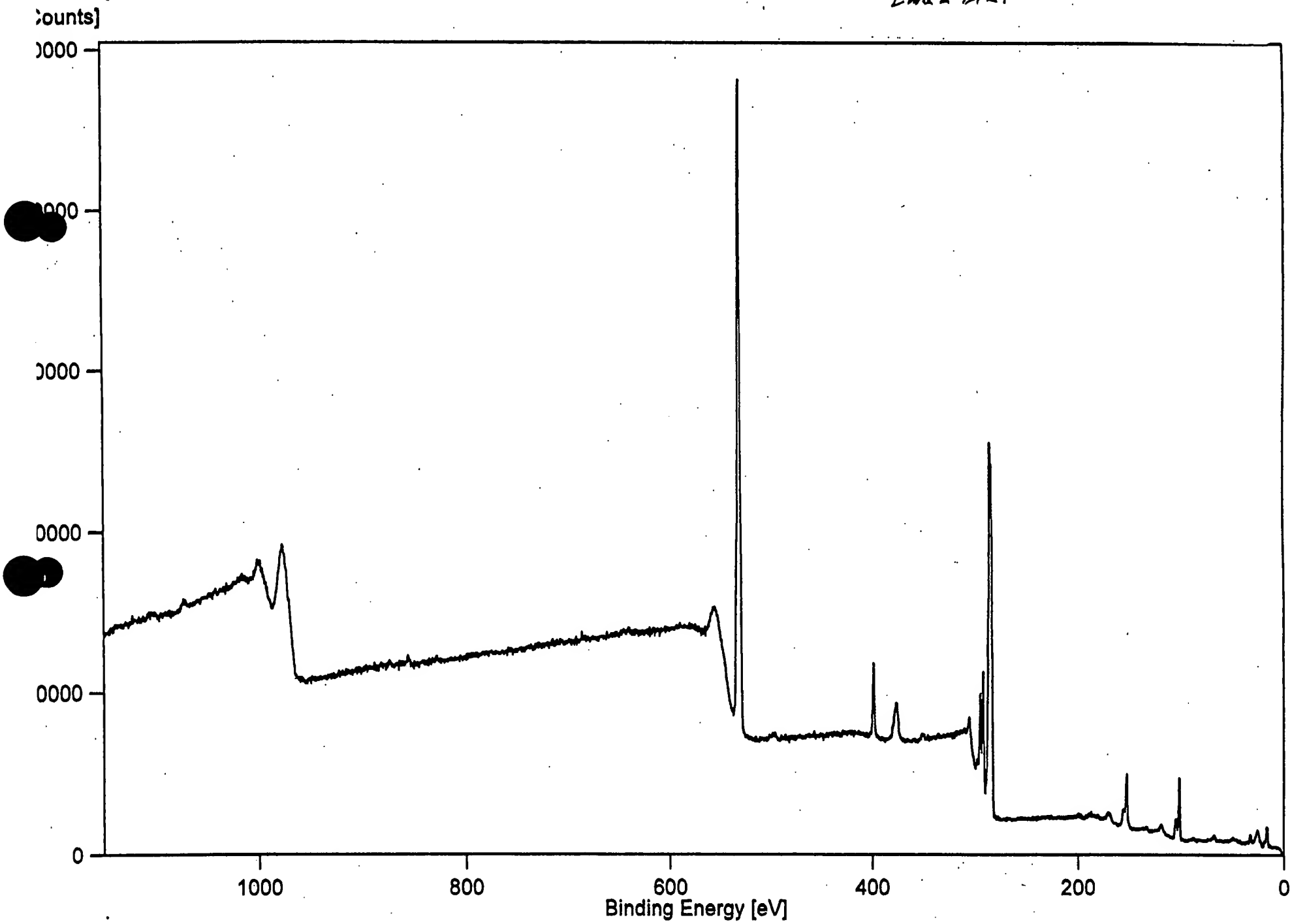
Counts]
0000
0000
0000
0000
0
1000
800
600
400
200
0
Binding Energy [eV]

Fig. 12

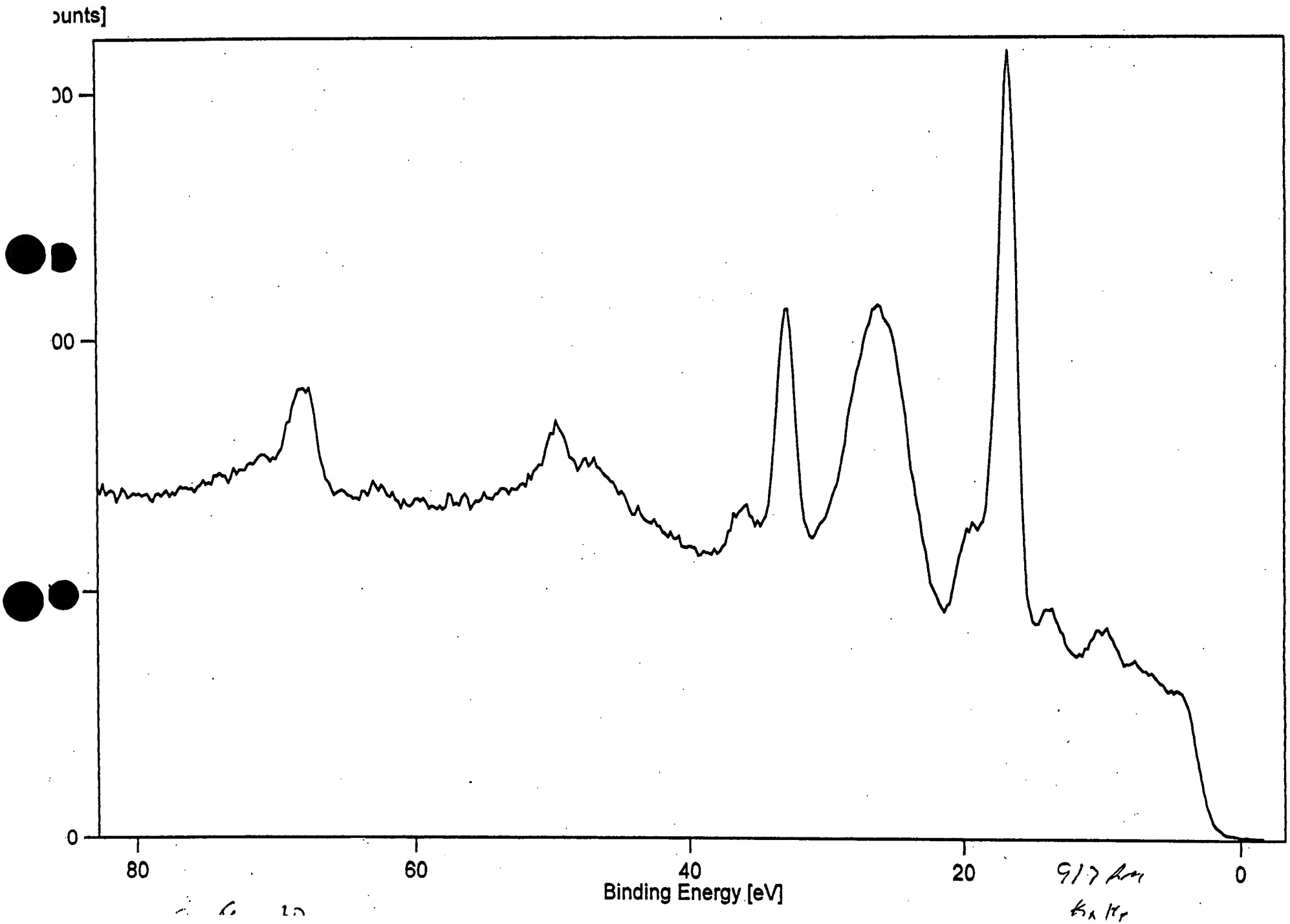

Fig. 13

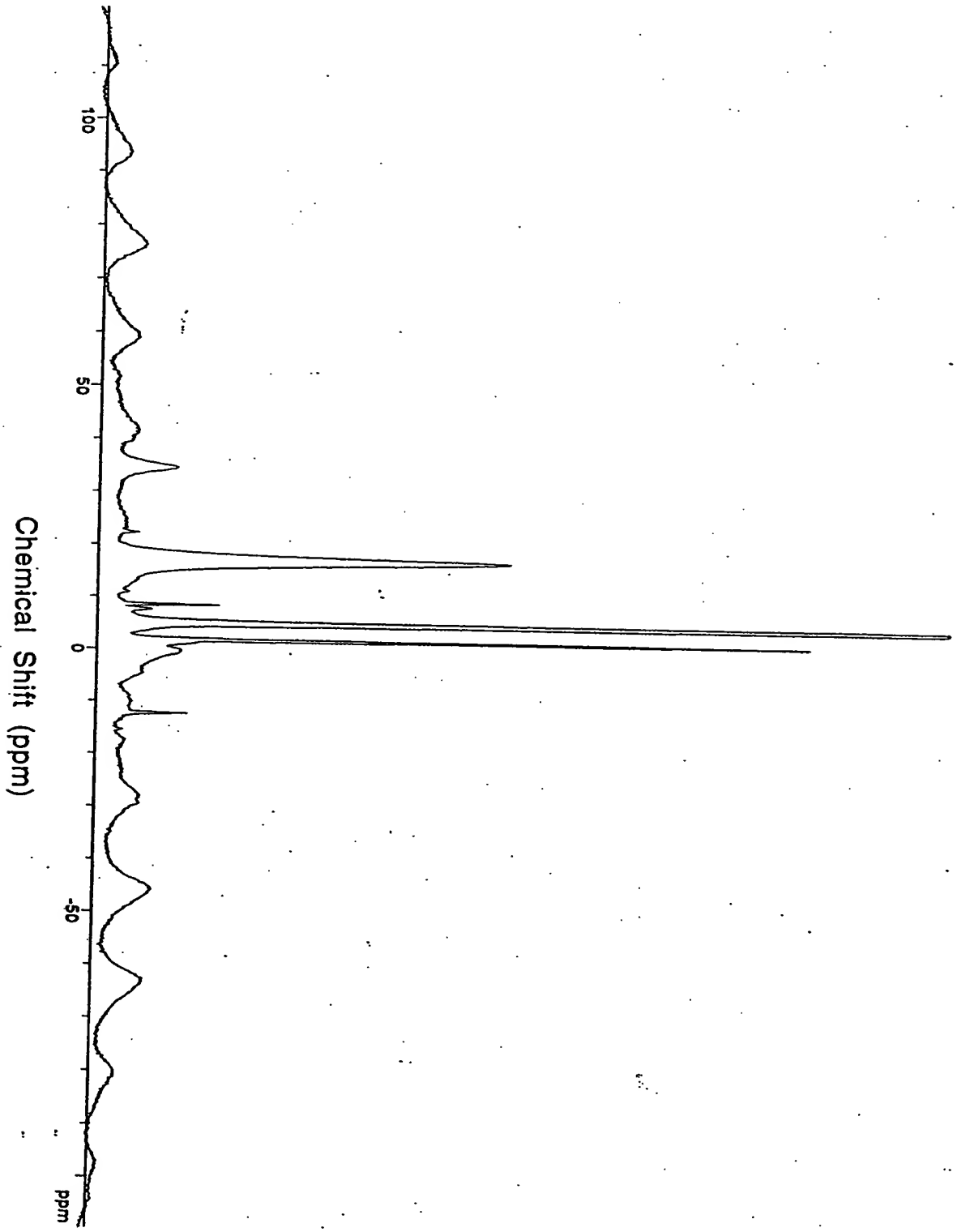

Fig. 14

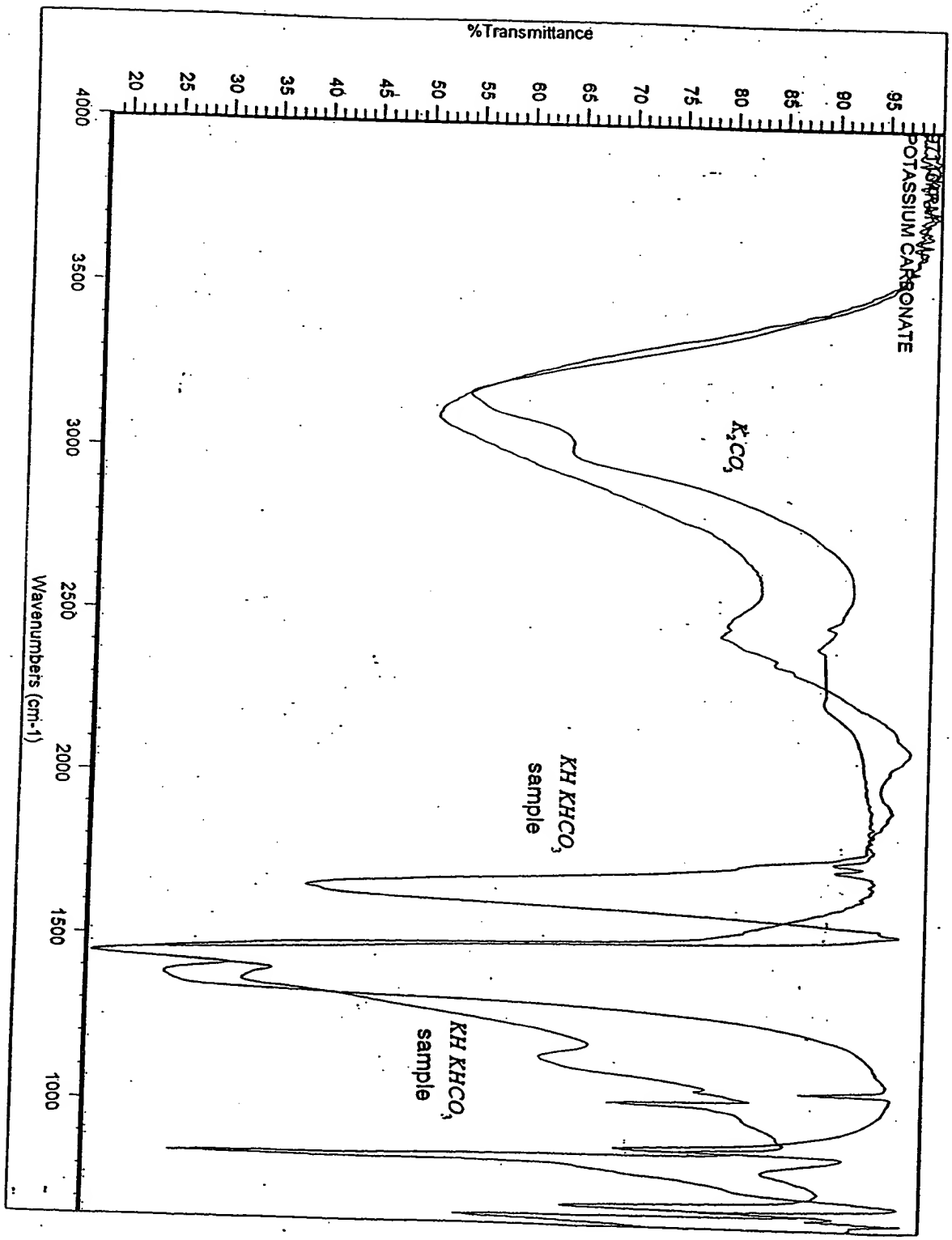
%Transmittance
Wavenumbers (cm-1)
POTASSIUM CARBONATE
K_2CO_3
KH $KHCO_3$ sample
KH $KHCO_3$ sample